CHAPTER 2

EXPERIMENTAL TECHNIQUES AND ALLIED THEORY

INTRODUCTION

Liquid crystal science has grown tremendously in recent years for fundamental scientific reasons and widespread applications in industry and technology e.g. display devices, optical devices and biological sensors etc. A large variety of materials have been synthesised and their properties have been determined, the scientists around the world are trying to develop and promote the ways to solve the problem of establishing the relationship among the properties of the molecules and the molecular structure of the substance, the macroscopic properties of the substance and the nature of the molecular motions. In this dissertation different properties of selected mesogenic compounds have been investigated employing various experimental techniques. Theoretical backgrounds of these techniques, in brief, along with the Maier-Saupe mean field theory explaining nematic-isotropic phase transition have been described in this chapter.

2.1 THEORIES OF LIQUID CRYSTALS IN BRIEF

Microscopic theoretical treatment of fluid phases may become quite complicated owing to the high material density, meaning that strong interactions, hard-core repulsions, and many-body correlations cannot be ignored. In the case of liquid crystals, anisotropy in all of these interactions complicates the analysis to a great extent. There are a number of fairly simple theories, however, that can at least predict the general behaviour of the phase transitions in liquid crystal systems. To explain and justify the liquid-crystalline phases, two basic theories are very helpful, the elastic continuum theory and the swarm theory. The continuum theory comprehends the liquid crystal as an anisotropic elastic medium with its own symmetry, viscosity and elasticity parameters [71]. This theory is a particularly powerful tool for modelling liquid crystal devices. In contrast the swarm theory interprets the state as the result of intermolecular interactions and the resulting statistical and thermodynamic equilibrium. In the elastic continuum theory, a molecular explanation of the macroscopically interpreted parameters is more or less given up, while in the swarm theory the molecular interaction forms the basis of the theory. The mathematical models of Oseen [72], Zocher [73] and Frank [71] contributed significantly in the development of these theories. The molecular statistical aspects was supported by the works of E. Bose [74], M. Born [75], R. C. Davis and G. W. Stewart[76], W. Maier and A. Saupe [77] along with Weiss' theory on magnetism and finally by the experiments of A. Smekal [78] and V. N. Tsvetkov [79]. Theoretical aspects of liquid crystals have been dealt with in details in, de Gennes and Prost's

monograph "The Physics of Liquid Crystals" [2], Chandrasekhar's monograph "Liquid Crystals" [3], Tsykalo's book "Thermophysical Properties of Liquid Crystals" [50] and by various other authors.

Molecular field method can be applied in developing a theory of spontaneous long-range orientational order and the associated properties of the nematic phase, nearly similar to that introduced by Weiss in ferromagnetism. Each molecule is assumed to be in an average orienting field due to its environment; however intermolecular short-range order and fluctuations are neglected. In 1916, Born proposed first molecular field theory for nematic state and treated the medium as an assembly of permanent electric dipoles and demonstrated the possibility of a transition from an isotropic phase to an anisotropic one as the temperature is lowered. But it is now well established that permanent dipole moments are not necessary for the occurrence of the liquid crystalline phase. The most extensively used treatment based on the molecular field approximation is that due to Maier and Saupe [77] which explains nematic-isotropic transition. Kobayashi [80] developed the first molecular statistical treatment of the smectic-nematic transitions introducing an additional isotropic paired intermolecular interaction in Maier-Saupe (MS) model. A similar but more specific approach was taken up by McMillan [81], who discussed the S_A-N transition in terms of the MS model considering orientational, translational and mixed order parameters. In the Kobayashi-McMillan theory also, the effects of short range order and fluctuation of the order parameters are neglected. The details of the McMillan, Wulf and de Gennes theories for SmC liquid crystals and the Meyer-McMillan theory for SmC, SmB and SmH liquid crystals are given in reference [50].

It might be worth to mention that thermotropic liquid crystals have also been extensively studied by computer simulation method employing a variety of hard, soft and realistic models involving atom-atom potentials and using either monte carlo or molecular dynamics method [82-90].

2.1.1 MAIER-SAUPE MEAN FIELD THEORY OF NEMATIC PHASE

An approach that has proved to be extremely useful in developing a theory of spontaneous long-range orientational order and related properties of the nematic phase is molecular field method. The most widely used treatment is that due to W. Maier and A. Saupe [77]. They developed the theory with the idea that the existence of the nematic phase is caused by the anisotropic part of the dispersion interaction energy between the molecules. The concept of an average potential is employed to all molecules since every molecule is

embedded in a 'sea' of many other molecules, the idea utilised in a thermodynamic system called a mean-field theory. It is assumed that each molecule is subjected to an average internal field that is independent of any local variations or short-range ordering. To find the exact nature of the intermolecular forces Maier-Saupe assumed that:

i) Molecules are rigid rods (spheroids, cylinders or spherocyliders) and rotationally symmetric with respect to their long molecular axes described by the unit vector **n**, called the director.

ii) With respect to a given molecule the distribution of the centre of mass of the remaining molecules may be taken to be spherically symmetric i.e., **n** and –**n** are equivalent.

iii) The influence of permanent dipoles can be neglected as far as long-range nematic order is concerned.

iv) Only the effect of the induced dipole-dipole interaction needs to be considered, the higher order terms are not thought to significantly affect the nematic order. No repulsive interaction is considered.

In nematic phase molecules possess only orientational ordering but no positional ordering. Degree of alignment of the molecules with respect to the director is described by an orientational order parameter

$$S = \langle P_2(\cos\theta_i)\rangle = \frac{1}{2}(3\langle\cos^2\theta_i\rangle - 1) \qquad 2.01$$

where θ_i is the angle between the long axis of the i^{th} molecule and the director **n**, statistical average is taken over all θ_i. In perfectly ordered state (crystalline state) θ_is are zero giving S=1, whereas in perfectly random state (isotropic liquid) average of $\cos^2\theta_i$ is 1/3 so that S=0. In nematic state, where ordering is in between crystalline and liquid state S will have values between 0 and 1.

Orientational dependence of the single molecule potential energy u is assumed to be functions of $\cos^2\theta_i$ as well as the degree of order of the system.

Thus

$$u_i(\cos\theta_i) \propto -\langle P_2(\cos\theta_i)\rangle\, P_2(\cos\theta_i)$$

or,

$$u_i(\cos\theta_i) = -\frac{A}{V^2}\langle P_2(\cos\theta_i)\rangle\, P_2(\cos\theta_i)$$

i.e

$$u_i(\cos\theta_i) = -v\langle P_2(\cos\theta_i)\rangle\, P_2(\cos\theta_i)$$

V is the volume of the sample and A is taken to be a constant characteristics of the molecule independent of pressure, volume and temperature.

Humphries, James and Luckhurst [91] developed a more comprehensive concept by including higher order terms in the mean field potential for cylindrically symmetric molecules. Thus u was taken as

$$u_i(\cos\theta_i) = \sum_{l \text{ even}} u_{li} \langle P_l(\cos\theta_i) \rangle P_l(\cos\theta_i) \qquad (l \neq 0) \qquad 2.02$$

where $P_l(\cos\theta)$ is the l^{th} order Legendre polynomial.

2.1.2 ORIENTATIONAL DISTRIBUTION FUNCTION AND EVALUATION OF THE ORDER PARAMETER

If the system be in thermal equilibrium then the probability of a molecule being oriented at an angle from the director **n** will be governed by the classical statistical mechanics, the theoretical orientational distribution function in terms of the mean field potential $u(\cos\theta)$ is given by

$$f(\cos\theta_i) = Z^{-1} \exp\left[\frac{-u_i(\cos\theta_i)}{kT}\right] \qquad 2.03$$

where k is the Boltzmann constant, T is temperature in absolute scale and Z is the partition function for a single molecule given by

$$Z = \int_0^1 \exp\left[\frac{-U(\cos\theta)}{kT}\right] d(\cos\theta) \qquad 2.04$$

where the subscript i has been dropped for brevity.

The order parameter S can therefore be written as

$$S = \langle P_2 \rangle = \int_0^1 P_2(\cos\theta) f(\cos\theta) d(\cos\theta)$$

$$= \frac{\int_0^1 P_2(\cos\theta) \exp[v < P_2(\cos\theta) > P_2(\cos\theta)/kT] d(\cos\theta)}{\int_0^1 \exp[v < P_2(\cos\theta) > P_2(\cos\theta)/kT] d(\cos\theta)} \qquad 2.05$$

where $T^* = kT/v$ is called the reduced temperature.

Thus for the determination of the temperature dependence of $\langle P_2(\cos\theta)\rangle$ we have a self-consistent equation. The value of $\langle P_2(\cos\theta)\rangle = 0$ is a solution at all T showing a disordered phase, the normal isotropic liquid. Also for $T^* < 0.22284$ two more solutions of $\langle P_2(\cos\theta)\rangle$ appear. One is positive $\langle P_2(\cos\theta)\rangle$ which tend to unity at T = 0 and represent the nematic phase. Other one is negative $\langle P_2(\cos\theta)\rangle$ which corresponds an unstable phase. The laws of thermodynamics state that the stable phase, will be the one having the minimum free energy. Applying this stability condition, we get the region $0 \leq T^* \leq 0.22019$, where $\langle P_2(\cos\theta)\rangle$ is greater than zero which corresponds an anisotropic nematic phase and for $T^* > 0.22019$, the isotropic phase with $\langle P_2(\cos\theta)\rangle = 0$ is the stable state.

The order parameter $\langle P_2(\cos\theta)\rangle$ varies from 1 at $T^* = 0$ to 0.4289 at $T^* = 0.22019$. Thus according to Maier-Saupe the transition from nematic to isotropic phase is first order which has been observed experimentally.

Exactly in similar way higher order parameter $\langle P_4(\cos\theta)\rangle$ can be obtained using the 4th order Legendre polynomial in equation (2.05).

$$\langle P_4(\cos\theta)\rangle = \frac{1}{8}(35 < \cos^4\theta > -30 < \cos^2\theta > +3) \qquad 2.06$$

The order parameter $\langle P_4(\cos\theta)\rangle$ varies from 1 at $T^* = 0$ to 0.1199 at $T^* = 0.22019$.

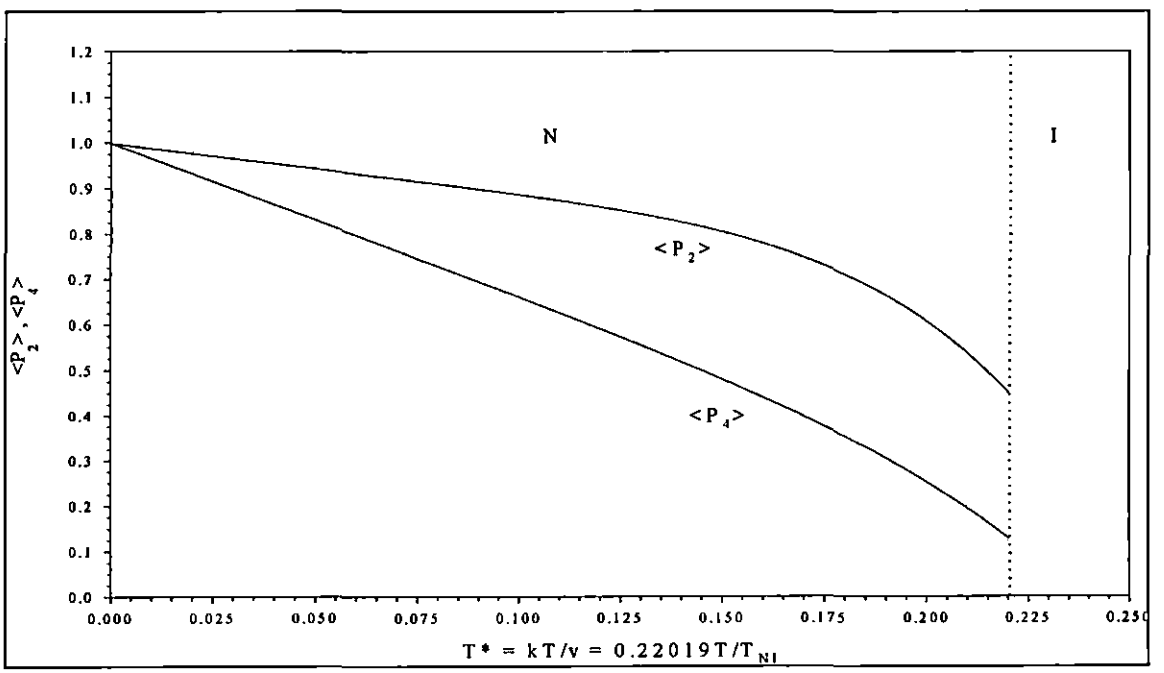

Figure 2.1. Order parameters $\langle P_2(\cos\theta)\rangle$ and $\langle P_4(\cos\theta)\rangle$ versus temp. from the Maier-Saupe theory.

Variation of $<P_2(\cos\theta)>$ and $<P_4(\cos\theta)>$ with temperature is shown in **Figure 2.1**. It is noted that nature of temperature variation of $<P_4(\cos\theta)>$ also indicate 1st order N-I transition.

The Maier-Saupe theory has also been extended to describe the smectic A- nematic transition in what is called McMillan's model [81] in which an additional order parameter for characterising the 1-D translational periodicity of a layered structure is included. Since the present dissertation is mainly related to the nematic phase of liquid crystals the detailed theory of smectic phases will not be discussed further.

2.1.3 THEORY OF X-RAY SCATTERING

The liquid crystal chemistry concentrate its focus on the relationship between molecular structure and properties of the various liquid crystal phases whereas liquid crystal physics focus on the mechanical, electrical, magnetic and optical properties of the various phases. There are different types of theoretical models that describe both LC phases and the transitions between the mesophases and the behaviour of liquid crystals in technical devices.

A quantitative explanation of a nematic phase is articulated in terms of an order parameter, which vanishes in isotropic phase. The great applicability of nematic liquid crystal in electro-optical devices is determined by its orientational order parameter and hence there is a sustained interest in these parameters computed using various methods are, (i) X-ray scattering [92-94], (ii) optical birefringence [95,96], (iii) the magnetic birefringence [97], (iv) NMR spectroscopy [97,98], (v) computer simulation [85-87, 89, 90] and dielectric spectroscopy [96]. Among the different approaches X-ray method has emerged as a powerful tool to compute the temperature variation of these orientational order parameters.

X-ray diffraction gives direct information about the residual positional order in liquid crystals. Bragg visualized the scattering of X-rays by a crystal in terms of reflections from sets of lattice planes, as shown in **Figure 2.2** (note that there is normally a phase change of 180^0 upon scattering, for X-rays).

For one particular set of planes, constructive interference between rays reflected by successive planes will only occur when the path difference, $2L_{hkl}\sin\theta$, equals an integral multiple of wavelength:

$$2L_{hkl}\sin\theta = n\lambda \qquad 2.07$$

where L_{hkl} is a periodicity in the sample and indices hkl refer to the Miller indices that indicate sets of planes in a certain direction and 2θ is angle of scattering. The width of the peaks depend obviously on the degree of long-range positional order. In liquids only short-

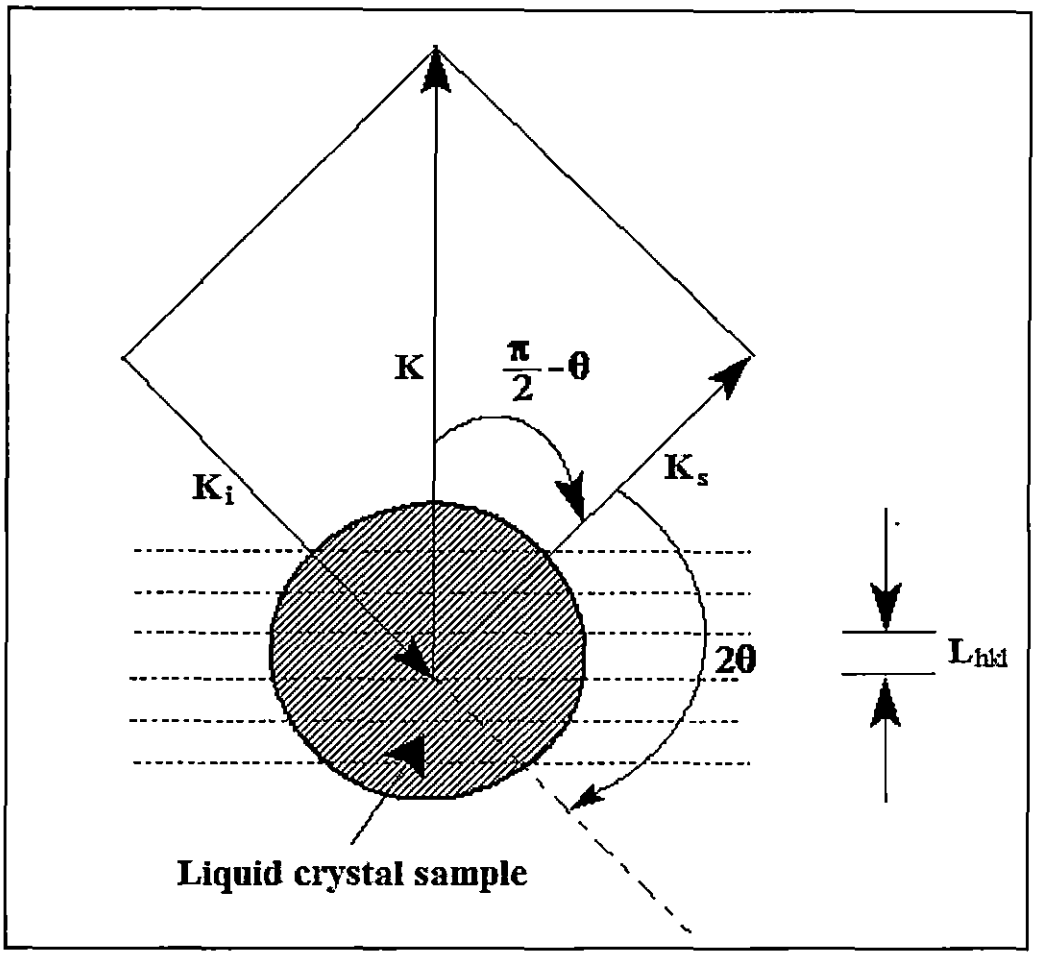

Figure 2.2. Typical scattering geometry showing the incident (K_i) and scattered (K_s) wave vectors.

range order is present and broad diffuse peaks will be observed. But in the nematic phase of mesogenic compounds the diffraction pattern consists of two diffuse rings. The inner ring at small Bragg angles is associated to the length of the molecules and the outer ring to the average lateral distance between neighbouring molecules. In the various smectic phases the random distribution in the longitudinal direction of the molecules is exchanged by a repeat distance corresponding to the spacing of the smectic layers.

To observe a particular diffraction peak, we must align the planes at an angle θ to the incident beam. The incident and diffracted beam directions are specified by their wave vectors $\mathbf{K}_i$ and $\mathbf{K}_s$. For elastic scattering, magnitude of incident and scattered wave vectors must be equal, i.e., $|\mathbf{K}_s| = |\mathbf{K}_i| = 2\pi/\lambda$. where λ is the wavelength of the incident radiation.

The magnitude of the scattering vector $\mathbf{K} = \mathbf{K}_s - \mathbf{K}_i$. is given by

$$K = |\mathbf{K}| = 4\pi\sin\theta/\lambda,$$

where 2θ is the angle between $\mathbf{K}_s$ and $\mathbf{K}_i$.. The scattering of incident radiation by a centre at **r** is described (relative to the initial amplitude) by the scattering amplitude

f exp(i**K**.**r**), where f is the scattering power. Generalised to N centres the scattering amplitude is written as

$$F(\mathbf{K}) = \sum_{j=1}^{N} f_j \exp(i\mathbf{K} \cdot \mathbf{r}_j) \qquad 2.08$$

where $\mathbf{r}_j$ denotes the position of scattering centre j. A further generalisation to a continuous distribution of scattering centres is the scattering amplitude

$$F(\mathbf{K}) = \int \rho(\mathbf{r}) \exp(i\mathbf{K} \cdot \mathbf{r}) d^3\mathbf{r} \qquad 2.09$$

where $\rho(\mathbf{r})$ is the time averaged electron density. For the case of isolated atom,q (2.09) can be written as

$$f(\mathbf{K}) = \int \rho_a(\mathbf{r}) \exp(i\mathbf{K} \cdot \mathbf{r}) d^3\mathbf{r}$$

and is called the atomic scattering amplitude. The above equation can be generalized to a group of atoms, for which

$$\rho(\mathbf{r}) = \sum_{j=1}^{N} \rho_j(\mathbf{r} - \mathbf{r}_j) \qquad 2.10$$

This leads to

$$F(\mathbf{K}) = \sum_{j=1}^{N} f_j(\mathbf{K}) \exp(i\,\mathbf{K} \cdot \mathbf{r}_j) \qquad 2.11$$

Equation (2.11) is nearly the same to equation (2.08). Therefore the diffraction by a set of atoms may be considered in terms of diffraction by a set of points, provided the variation of the atomic scattering amplitude is accounted for.

To get absolute value and hence the experimentally related intensity, the amplitude of a wave scattered by a single point electron must be known. With the help of classical electrodynamics expressing all intensities in terms of the scattering intensity of an electron we get expression for intensity

$$I(\mathbf{K}) = |F(\mathbf{K})|^2$$

It is convenient for molecular liquids to separate the amplitude due to the molecular structure from the total scattering amplitude [99]. Accordingly (2.11) can be written as

$$F(\mathbf{K}) = \sum_{k,m} f_{km}(\mathbf{K}) \exp[i\mathbf{K} \cdot (\mathbf{r}_k - \mathbf{R}_{km})] \qquad 2.12$$

where $\mathbf{r}_k$ gives the position of the centre of mass of the k^{th} molecule and $\mathbf{R}_{km}$ is the position of the m^{th} atom in the k^{th} molecule, f_{km} is the atomic scattering factor of the m^{th} atom in the k^{th} molecule.

Therefore the general formula for the intensity of scattering from a system of molecules is

$$I(\mathbf{K}) = \sum_{k,l,n,m} \langle f_{km}(\mathbf{K}) f_{ln}^{*}(\mathbf{K}) \exp[i\mathbf{K}.(\mathbf{r}_k - \mathbf{r}_l)] \exp[i\mathbf{K}.(\mathbf{R}_{ln} - \mathbf{R}_{km})] \rangle \qquad 2.13$$

where the < > indicates statistical average over all the molecules of the system.

The intensity can be written as

$$I(\mathbf{K}) = I_m(\mathbf{K}) + D(\mathbf{K})$$

where $I_m(\mathbf{K})$ is the molecular structure factor and $D(\mathbf{K})$ is called the interference function are given by

$$I_m(\mathbf{K}) = \sum_k \langle \sum_{m,n} f_{km}(\mathbf{K}) f_{kn}^{*}(\mathbf{K}) \exp[i\mathbf{K}.(\mathbf{R}_{kn} - \mathbf{R}_{km})] \rangle$$

$$= N \langle \left| \sum_m f_{km} \exp\left(-i\mathbf{K}.\mathbf{R}_{km}\right) \right|^2 \rangle \qquad 2.14$$

and

$$D(\mathbf{K}) = \langle \sum_{k \neq l}^{m} \exp(i\mathbf{K}.\mathbf{r}_{kl}) \sum_{m,n} \langle f_{km}(\mathbf{K}) f_{ln}^{*}(\mathbf{K}) \exp[\mathbf{K}.(\mathbf{R}_{ln} - \mathbf{R}_{km})] \rangle \qquad 2.15$$

where $\mathbf{r}_{kl} = \mathbf{r}_k - \mathbf{r}_l$ .The term $I_m(\mathbf{K})$ gives the scattered intensity which would be observed from a random distribution of identical molecules.

$D(\mathbf{K})$ is the term containing information about correlation in both positional and orientation of different molecules. In other words it contains the information regarding, (i) Apparent molecular length, (ii) Layer thickness in smectics, (iii) Average lateral distance between the molecules, (iv) Tilt angle, (v) Orientational distribution function, (vi) Order parameters (vii) correlation lengths etc.

2.2 IDENTIFICATION OF PHASES

As discussed in section **1.2** there are many different types of liquid crystal phases and in many cases the distinction between two phases is very subtle. The identification of liquid crystal phase type is, therefore, usually done by several techniques which are complimentary to each other viz., (i) Differential scanning calorimetry (DSC), (ii) Optical polrization microscopy (OPM), (iii) Miscibility study and (iv) X-ray Diffraction etc. Of these, X-ray diffraction is the most useful technique to find the microscopic structure of liquid crystals. It reveals the nature of distribution of molecules within the phase and thus the phase type can be identified uniquely.

2.2.1 DIFFERENTIAL SCANNING CALORIMETRY (DSC)

Differential Scanning Calorimetry (DSC) discloses the presence of phase transitions in a material by detecting the enthalpy change associated with each phase transition. The schematic setup of DSC is shown in **Figure 2.3**. The level of enthalpy change gives some

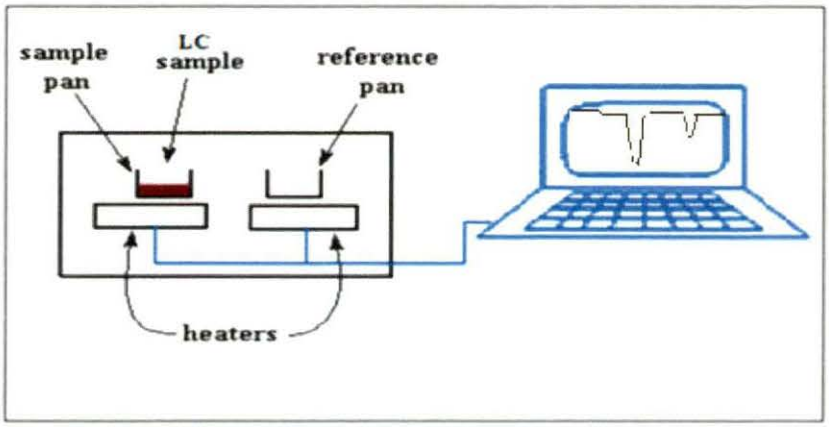

Figure 2.3. *Schematic setup of differential scanning calorimetry studies.*

information about the degree of molecular ordering within a mesophases, indicating the types of phase involved. Accordingly DSC is used in conjunction with OPM to conclude the type of mesophases. When a material melts, a change of state occurs from solid to liquid and this melting process requires energy (endothermic) from the surroundings. Converse is also true. The DSC instrument measures the energy absorbed or released by a sample as it is heated or cooled. Solid to liquid involves high energy of transition (enthalpy change around 30 to 40

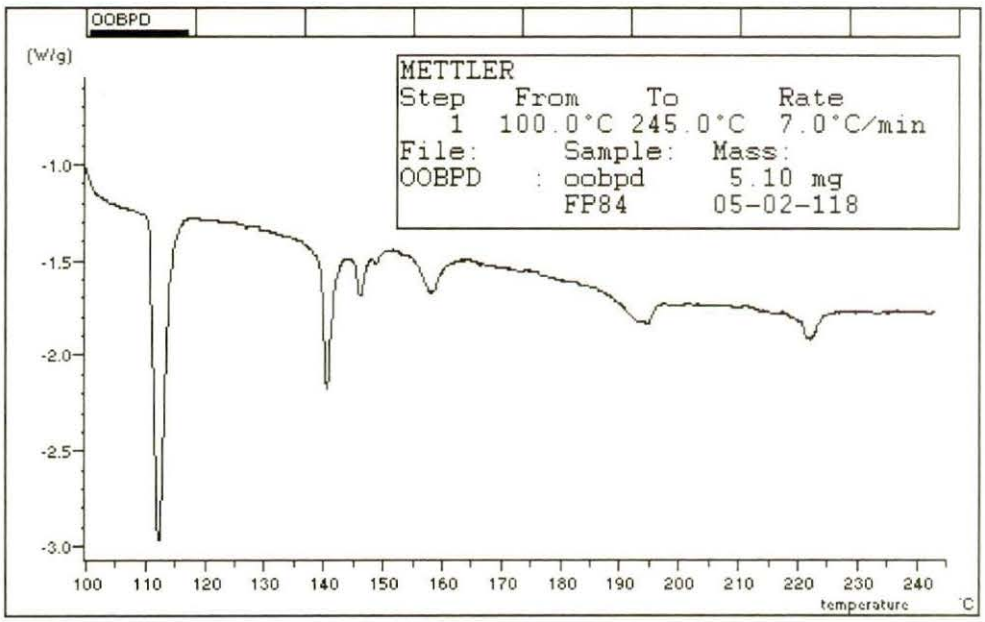

Figure 2.4. *DSC plot of OOBPD {Bis-(4,4/-n-alkoxy-benzylidene)-1,4-phenylenediamines} sample [100].*

$kJmol^{-1}$). But more subtle structural phase changes are involved within liquid crystalline phases which are reflected by the relatively small enthalpy changes (1 to 2 $kJmol^{-1}$). Usually crystal to N or SmA transitions and N or SmA to isotropic transitions are first order although liquid crystal to isotropic liquid transition is less prominent than crystal to liquid crystal phase transition. But crystal to higher order smectics (like SmG) and liquid crystal to liquid crystal phase changes are weakly first order or second order in nature and not always detectable by DSC techniques. We used Mettler FP82 hot stage and FP84 thermosystem for texture and DSC studies. Typical DSC plot for one of the investigated compound is shown in **Figure 2.4,** which has 4 different smectic phases (S_H, S_G, S_I and S_C) along with nematic phase [100].

2.2.2 OPTICAL POLARISING MICROSCOPY (OPM)

The optical polarising microscopy is the most commonly used tool for identification of phases present in a newly synthesized mesogenic material. The most remarkable feature of liquid crystals is the wide variety of visual patterns they display under polarised light as shown in **Figure 2.5**. These visual patterns, called textures, are due almost entirely to the defect structure that occurs in the long-range molecular order of the liquid crystals materials. The identification of mesophases through OPM typically involves observation of the magnified view of a thin sample (thickness ~ 10-20 μm) sandwiched between a microscope slide and a glass cover slip under crossed polarizers. The temperature of the material is controlled by placing it in a hot stage, temperature of which can be varied from room temperature to usually up to 300°C. In isotropic phase the field of view appears dark, but beautiful texture appears if the material form liquid crystal phase on cooling. Observed texture type depends on the alignment of the sample viz., whether homeotropic or homogeneous (planar) and the involved phase structure.

In homeotropic alignment the molecular long axes (optic axes) are oriented normal to the supporting substrate. When the molecules are so oriented polarised light is unaffected by the material and so light cannot pass through the analyser showing complete blackness.

In homogeneous (planar) alignment the constituent molecules of the liquid crystals phase are oriented parallel to the supporting substrates. In this case, a thin aligned layer of the liquid crystals phase exhibits birefringence and a coloured texture results when viewed between crossed polarisers.

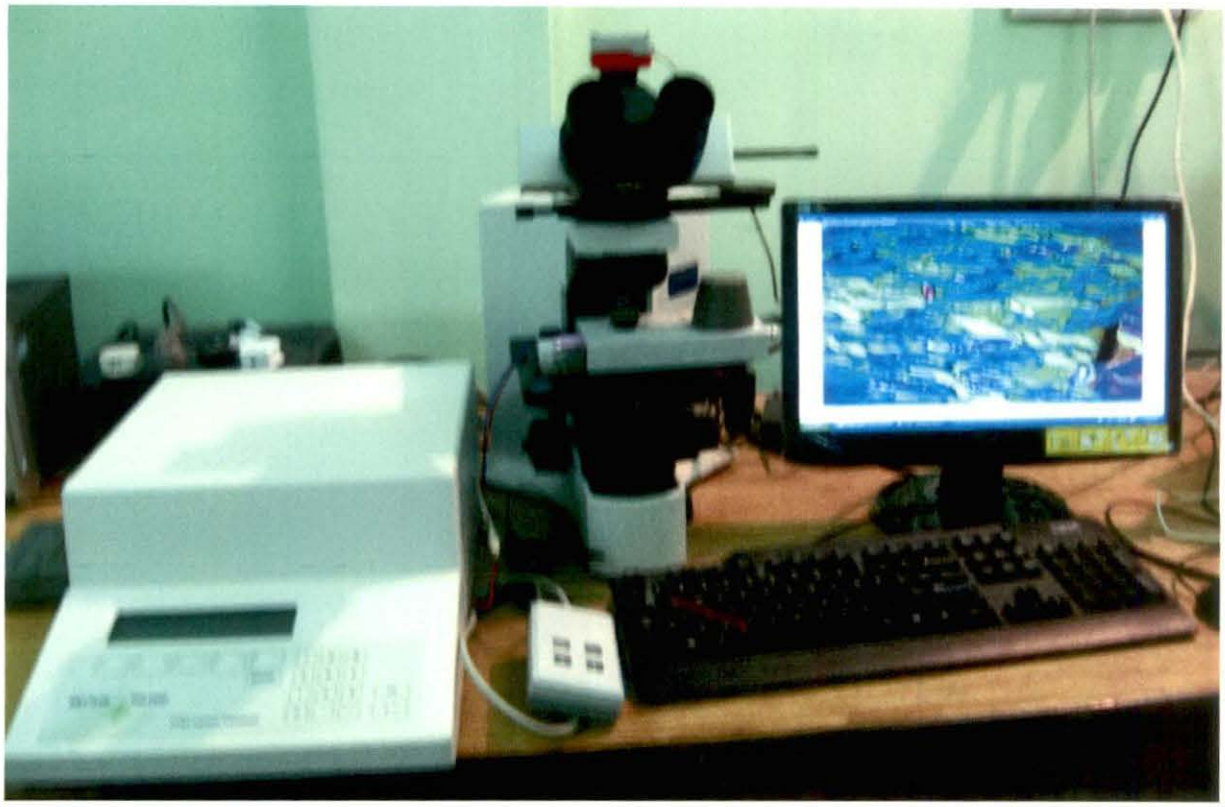

Figure 2.5. *Experimental setup of a polarizing microscope as used for texture studies.*

However, the identification of the mesophases by this technique is often difficult because similar textures might be exhibited by different phases or sometimes very subtle change in textures occur at transitions and hence requires the support of other techniques to finalize the phase type present. Typical textures observed in various phases are described in several books [101-104].

2.2.3 TECHNIQUES FOR X-RAY DIFFRACTION STUDIES AND METHOD OF DATA ANALYSIS

X-ray diffraction is the most reliable technique for investigating the microscopic structure of liquid crystals. It maps the positions of the molecules within the phase and hence determines the phase structure and classification to which the particular phase belongs. However for getting better information good quality photograph from aligned samples are needed. Alignment of the sample, which is usually done by the application of magnetic field, is difficult especially for higher order smectic phases.

Experimental set-up used for X-ray diffraction studies was designed and fabricated in our laboratory earlier [105,106]. Small and wide angle X-ray photographs were taken throughout the mesomorphic range using Nickel-filtered CuK_{α} radiation, the temperature was

regulated within ±0.5°C by a controller, Indotherm 401-D2, later the Eurotherm controller (2216e) was also used for controlling the temperature with an accuracy ±0.1°C.

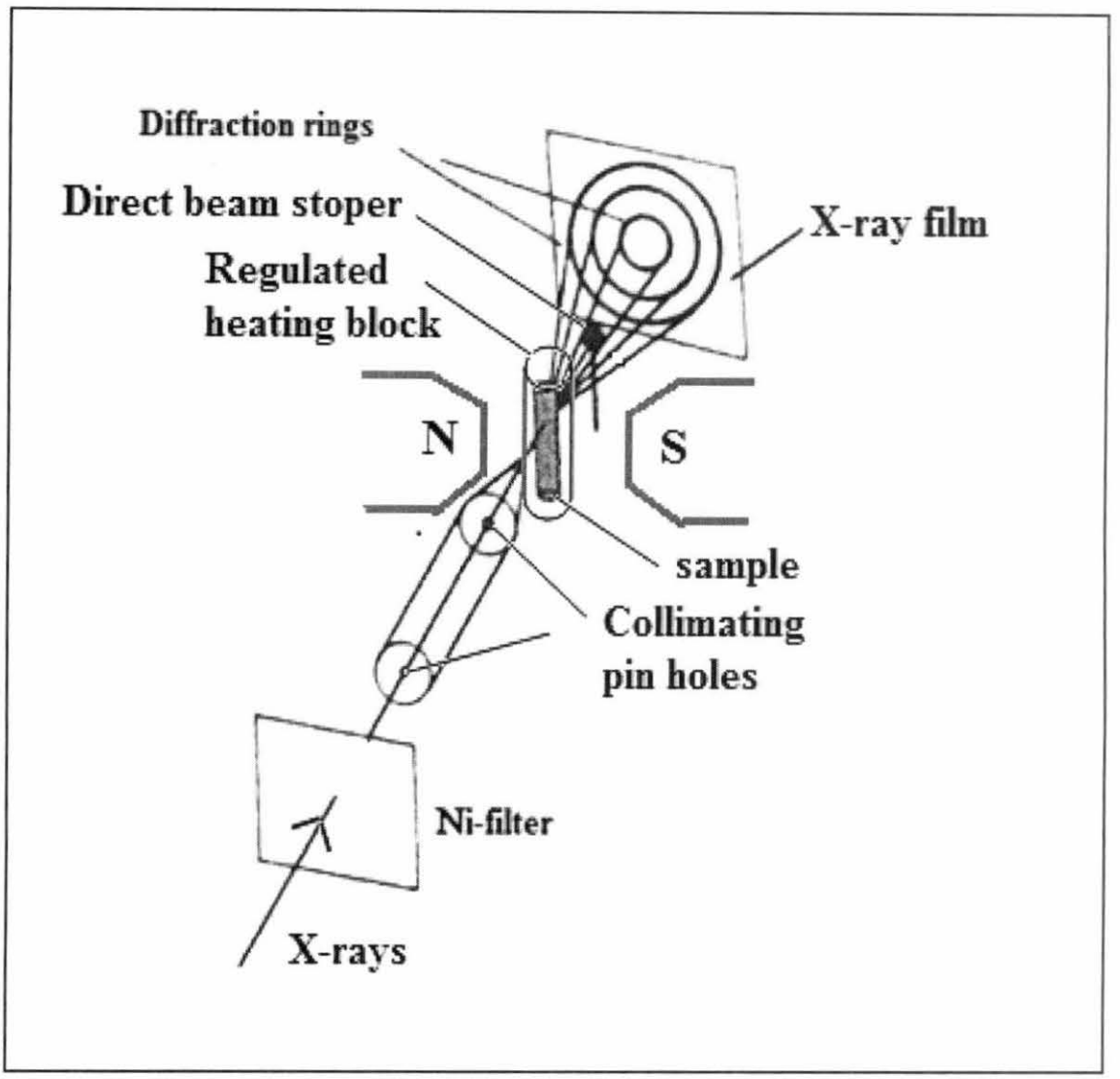

Figure 2.6. *Schematic diagram of the flat film camera.*

Essential features required in the set up for recording X-ray diffraction pattern of a liquid crystal on a flat film camera are shown schematically in **Figure 2.6**. Collimated Ni-filtered CuK_{α} radiation was made incident on the sample taken in a thin walled glass capillary. Sample was introduced by capillary action in isotropic state and then cooled slowly to the desired temperature in presence of magnetic field of about 4-5 KG. All photographs were taken with X-rays perpendicular to the magnetic field direction. Various types of diffraction patterns are obtained depending upon the type of the mesophases [107-116]. Schematic representation of magnetically aligned sample by X-ray scattering of nematic and smecticA liquid crystals are shown in **Figure 2.7(a)** and **Figure 2.7(b)** respectively.

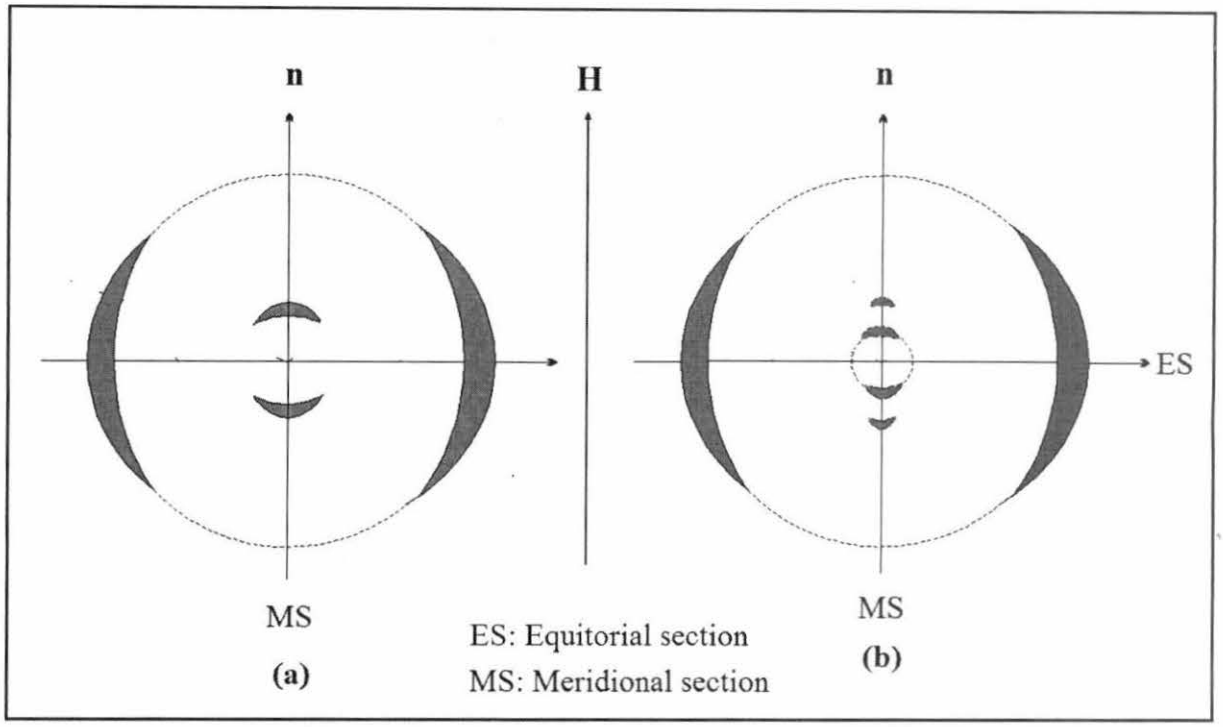

Figure 2.7. *Schematic representation of the X-ray diffraction pattern of an oriented* ***(a)*** *nematic and* ***(b)*** *smectic A phase.*

In the diffraction pattern two characteristic features, parallel and perpendicular to **n** (or **H**) are observed. X-ray diffraction pattern has a symmetry of revolution around the direction of X-ray beam. For unaligned nematic/smectic phase two uniform halos, just like that from an isotropic liquid, are obtained. However, the outer circular halo of an oriented nematic sample is splitted into two crescents showing maxima along the equatorial direction perpendicular to **n** as shown in **Figure 2.7(a)**, which are formed due to intermolecular scattering and the corresponding diffraction angle gives a measure of average lateral intermolecular distance (D). Generally these distances lie between 3.5Å and 6.5Å, lateral dimension of a typical mesogenic molecules.

Inner halo also has two crescents with maxima at much lower angle in the meridional direction parallel to **n** (or **H**). This diffraction peak must arise from correlations in the molecular arrangement along **n**. So by measuring the corresponding angles of diffraction one gets the value of the apparent molecular length (*l*) in the nematic phase. In case of smectic phases the inner pattern appears as sharp spots, sometimes second order spots are also found. Diffraction angle corresponding to 1^{st} order spots arises due to smectic layer spacing, from the 2^{nd} order spots the translational order parameter can also be determined.

Using Bragg equation $l = \lambda/2\sin\theta$ the apparent molecular length (l) for nematic phase and layer thickness for smectic phase (d) are calculated but the average intermolecular distance (D) are determined using a modified Bragg formula $D=1.117\lambda/2\sin\theta$ derived by de Vries [117,118] on the arguments of cylindrical symmetry. Bragg angle θ was determined from the relation,

$$\tan 2\theta = \frac{\text{Radius of the ring}}{\text{sample to film distance}} \qquad 2.16$$

where sample to film distance was found from the (111) and (222) reflections of aluminium powder.

For the above analysis the X-ray photographs were scanned by using a scanner (hp scan jet 2200c). The digitized images were analyzed using the colour values of the pixels to obtain the radii of the inner and outer diffraction rings. Two softwares, Adobe Photoshop 7.0 and origin 7.0 were used for analyzing the digital images.

Orientational distribution function $f(\theta)$ and orientational order parameters $\langle P_L \rangle$ were calculated from the azimuthal intensity profile of equatorial arcs in the X-ray diffraction pattern, following a procedure described below.

By circular scanning of the photograph at an interval of 5 degrees, azimuthal distribution of colour values along the equatorial arc is determined and $\Psi=0^\circ$ is taken at the minima of the colour values, i.e. along meridional direction. These colour data (**Figure 2.8**) are converted to intensity using a calibration curve and following the procedure of Klug and Alexander [119].

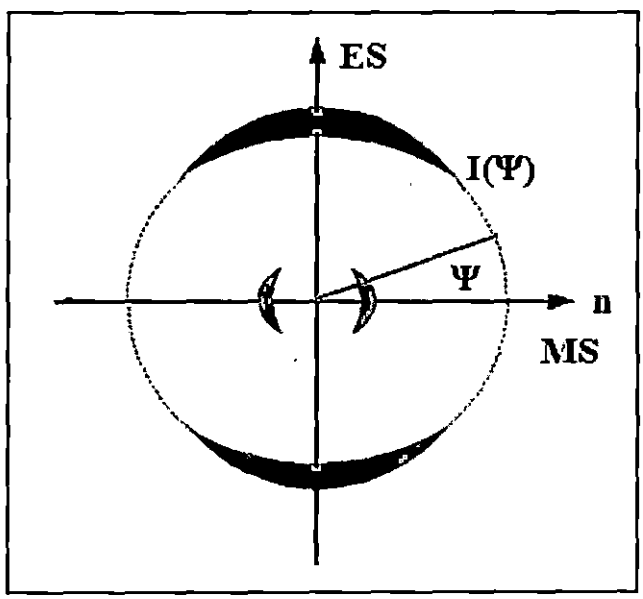

Figure 2.8. *Schematic representation of colour data for X-ray diffraction pattern of an oriented a nematic phase.*

The experimental intensity values were then corrected for background intensity values arising due to the air scattering. Thus we get angular intensity distribution I(Ψ) as a function Ψ as shown in **Figure 2.9.** In order to find the orientational distribution function f(θ) from the intensity distribution I(ψ) following relation, given by Leadbetter and Norris[94], was used.

$$I(\psi) = C\int_{\theta=\psi}^{\pi/2} f(\theta)\sec^2\psi\left[\tan^2\theta - \tan^2\psi\right]^{-1/2}\sin\theta d\theta \qquad 2.17$$

f(θ) was calculated following the procedure described by Bhattacharjee et al. [93]. As molecular distribution in the nematic phase is centrosymmetric, the distribution function and the intensity can be expanded as even cosine power series.

$$I(\psi) = \sum_{n=0}^{r} a_{2n}\cos^{2n}\psi \qquad 2.18$$

$$f(\theta) = \sum_{n=0}^{r} b_{2n}\cos^{2n}\theta \qquad 2.19$$

Both the series converge rapidly. Retaining eight terms in the truncated series, a least square fitting was made with the observed I(ψ) values to get the coefficients a_{2n}, from which the coefficients of b_{2n} were calculated using the relation

$$b_{2n} = a_{2n}\frac{(2n+2)!}{2^{2n}(n!)^2} \qquad 2.20$$

In this way one can find the orientational distribution functions from the measured intestity distribution of intensity.

Orientational order parameter $\langle P_2\rangle$ and $\langle P_4\rangle$ were then calculated using the following equation

$$\langle P_L\rangle = \frac{\int_0^1 P_L(\cos\theta)f(\theta)d(\cos\theta)}{\int_0^1 f(\theta)d(\cos\theta)} \qquad 2.21$$

Necessary computer program was developed for this purpose in our laboratory. The uncertainties in calculated *I* and D values are ± 0.1, ± 0.02 respectively and that in $\langle P_2\rangle$ and $\langle P_4\rangle$ values are estimated to be ±0.02.

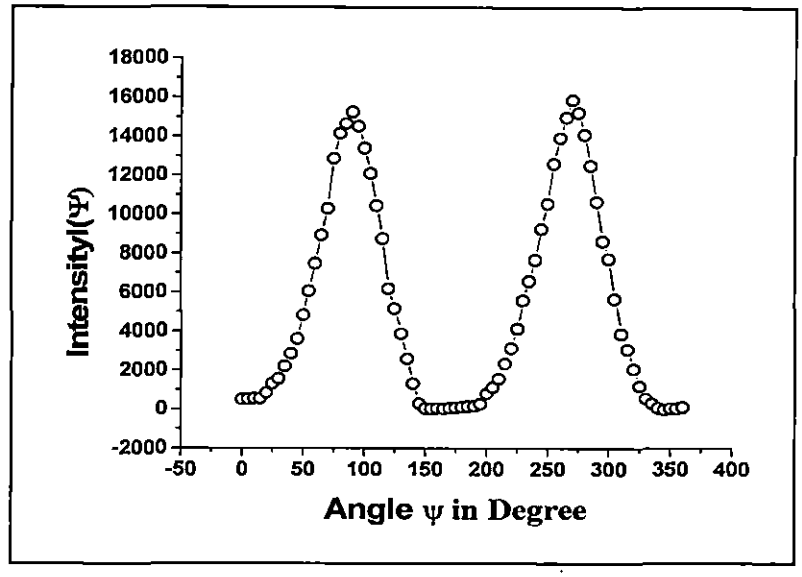

Figure2.9. The angular intensity distribution I(Ψ) vs. angle (Ψ) curve.

2.3 STUDY OF BIREFRINGENCE PROPERTY

When light propagates through a material, its wavelength and velocity decreases by a factor which is known as refractive index of the medium. An isotropic liquid has single refractive index since light polarised in any direction travels at the same velocity. In non-magnetic materials, the index of refraction, according to Maxwell's theory, is equal to square root of relative permittivity or dielectric constant. Since the relative permittivity is different for electric fields in different directions the refractive index is also different. This optical phenomena is called birefringence. The birefringence (Δn) is defined as the difference between the extraordinary ray refractive index (n_e) and the ordinary ray refractive index (n_o) i.e. $\Delta n = n_e - n_o$. The first one, the extraordinary refractive index n_e is observed, when the electric vector of the incident beam is parallel to the optic axis of the molecule whereas n_o is observed when electric vector is perpendicular to the optic axis. The optical anisotropy or birefringence depends on the wavelength of the light and the thermal state of the compounds [120]. Physical origin of the optical properties of liquid crystal has been discussed in detail by Dunmur [121].

The molecular polarizability (α) of the molecules and order parameter control the optical anisotropy. The linear molecules having a long and rigid core exhibit high order parameter. Molecules that consist of high polarizability units (having π and delocalized electrons) such as aromatic rings in the core, tolane linking groups and terminal cyano groups have a high birefringence. Conversely, a low birefringence is exhibited by molecules that are deficient in these types of groups and usually consist of alicyclic groups and terminal alkyl chains. The molecular polarizability 'α' can be determined if the value of

internal field, i.e., the average field acting on an individual molecule is known. Lorenz-Lorentz field, commonly known internal field valid for isotropic phase, is not applicable for mesogenic systems. Therefore, more realistic internal field, proposed by the Vuks'[122] and Neugebauer's [123] are usually applied in liquid crystalline systems.

2.3.1 MOLECULAR POLARIZABILITIES FROM REFRACTIVE INDEX

* *VUKS' METHOD*

Vuks' derived the relations for polarizabilities associated with anisotropic molecules, considering the internal field as independent of molecular interaction. In this case the principal molecular polarizabilities α_o and α_e, perpendicular and parallel to the direction of optic axis, are related to n_o and n_e by the following equations:

$$\alpha_o = \frac{3}{4\pi N}\frac{n_o^2-1}{n^2+2} \qquad 2.22$$

$$\alpha_e = \frac{3}{4\pi N}\frac{n_e^2-1}{n^2+2} \qquad 2.23$$

where N is the number of molecules per unit volume obtained from density and n is the average refractive index and is given by $n=1/3\ (n_e+2n_o)$.

* *NEUGEBAUER'S METHOD*

Lorenz-Lorentz equations for an isotropic system was extended by Neugebauer by representing the polarizability of a molecule by an anisotropic point polarizability and showed that

$$n_e^2 - 1 = 4\pi N\alpha_e\left(1-N\alpha_e\gamma_e\right)^{-1} \qquad 2.24$$

$$n_o^2 - 1 = 4\pi N\alpha_o\left(1-N\alpha_o\gamma_o\right)^{-1} \qquad 2.25$$

where γ_e and γ_o are the respective internal field constants for extraordinary and ordinary rays. Above equations can be rewritten in the following form:

$$\frac{1}{\alpha_e}+\frac{2}{\alpha_o} = \frac{4\pi N}{3}\left[\frac{n_e^2+2}{n_e^2-1}+\frac{2\left(n_o^2+2\right)}{n_o^2-1}\right] \qquad 2.26$$

$$\alpha_e + 2\alpha_o = \frac{9}{4\pi N}\left[\frac{n^2-1}{n^2+2}\right] \qquad 2.27$$

Principal polarizabilities can be obtained by solving the above two equations.

2.3.1.1 ORDER PARAMETERS (<P_2>) FROM POLARIZABILITIES

The principal polarizabilities, parallel and perpendicular to the direction of optic axis, are related to the orientational order parameter <P_2> of nematics [3, 124] by the following relations,

$$\alpha_e = \overline{\alpha} + \frac{2}{3}\Delta\alpha\langle P_2\rangle$$

and

$$\alpha_o = \overline{\alpha} - \frac{1}{3}\Delta\alpha\langle P_2\rangle$$

Therefore orientational order parameter

$$\langle P_2\rangle = \frac{\alpha_e - \alpha_o}{\alpha_{\parallel} - \alpha_{\perp}} \qquad 2.28$$

where, $\overline{\alpha} = (2\alpha_o + \alpha_e)/3$, is the mean polarizability and $\Delta\alpha = \alpha_e - \alpha_o$ is the polarizability anisotropy. $\alpha_{\parallel}$ and $\alpha_{\perp}$ are the principal polarizabilities parallel and perpendicular to the long axes of the molecules in the perfectly ordered crystalline state where <P_2> =1 which are, however, not easily measurable.

The widely used Haller's extrapolation method is adopted [125] for getting the values of $(\alpha_{\parallel} - \alpha_{\perp})$ in the solid state. A graph is plotted with log $(\alpha_e - \alpha_o)$ vs. log $(T_c - T)$ which should be a straight line. Extrapolating the straight line up to log (T_c) one obtains the value of $\alpha_{\parallel} - \alpha_{\perp}$. Here T_C corresponds to the N-I transition temperature.

2.3.1.2 MEASURING TECHNIQUE FOR REFRACTIVE INDICES

The refractive indices corresponding to the ordinary (n_o) and extraordinary (n_e) rays, were measured by thin prism technique. Using two optically flat glass plates thin prisms were prepared, following a procedure described by Zeminder et al [126]. Initially the glass plates were cleaned by nitric acid and washed thoroughly with distilled water. Finally washing with acetone, the glass plates were dried and then treated with a dilute solution of polyvinyl alcohol to develop a thin layer on the treated glass plate using spin coater. The preferred direction on the substrates was obtained by rubbing the coated glass plates several times in the same direction on a bond paper. The prism was then formed, by keeping the treated surfaces

inside and the rubbing directions parallel to the refracting edge of the prism. Using high temperature adhesive three sides of the prism was sealed. Generally the angles of the prisms are kept less than 1° by using a thin glass spacer. The prisms were then left to dry and then baked for several hours. The sample was introduced inside the prism by melting a few crystals, at the top of the open side. Repeated heating and slow cooling produced a

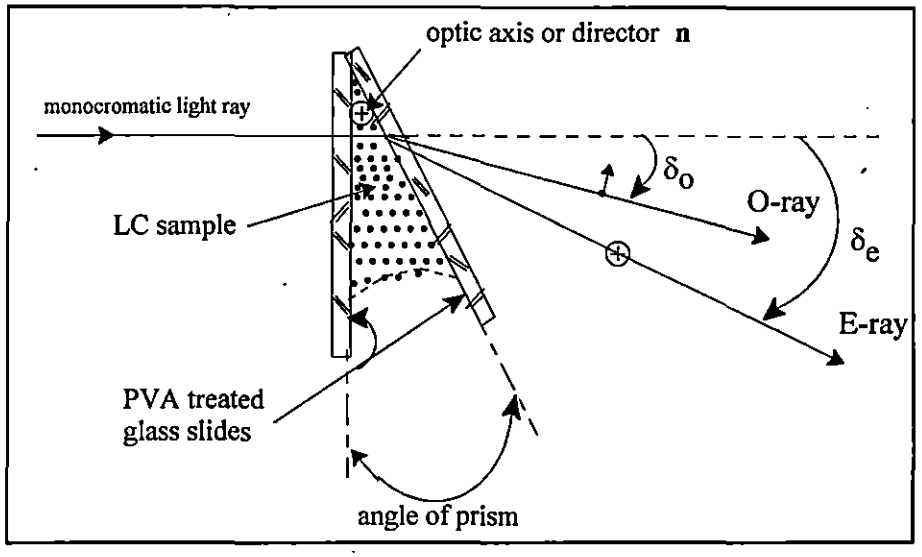

Figure 2.10. Schematic arrangement for the measurement of refractive indices.

homogeneous sample with the molecules perfectly aligned having the optic axis parallel to the refractive edges. The prism was then placed inside a thermostated brass oven with a circular aperture. The temperature of the oven was controlled by a temperature controller (Indotherm model 401 with an accuracy of ± 0.5°C (Eurotherm model 2216e with an accuracy of ±0.1°C). The refractive indices were measured by using a mercury lamp, a polarizer, a nicol prism, a wavelength selector and a precision spectrometer, for the wavelengths 5461Å (λ_G), 5780(λ_Y) and 6907 (λ_R) corresponding to the green, yellow and red light respectively with an accuracy ±0.1%. A schematic representation of the experimental set up for the measurements of refractive indices is shown in **Figure 2.10**.

2.4 MEASUREMENT OF DENSITY

Using a glass tube dilatometer of capillary type, a travelling microscope and temperature controller, the density of samples was measured. The bulb of the dilatometer was filled with mercury. A weighed sample of the liquid crystal was then introduced inside the dilatometer in isotropic state. The loaded dilatometer was placed in a thermostated silica oil

bath. Sufficient time was allowed to reach the equilibrium at the desired temperature before taking each reading. The length of the liquid crystal column was measured at different temperatures during cooling from the isotropic state, with a travelling microscope. The densities were calculated after making the correction for expansion of glass. Accuracy of measured density was ± 0.1%.

2.5 DIELECTRIC PERMITTIVITY OF MESOPHASES

From the studies of dielectric properties of nematic liquid crystals one gets number of valuable information on molecular organisation, intermolecular interactions and molecular dynamics in both the mesomorphic and isotropic phases. The study of the temperature dependence of the permittivity of liquid crystals has also considerable practical importance. The threshold voltage and other operational parameters of liquid crystal displays depend on the anisotropy of the permittivities and the multiplexity of matrix displays may be limited by the temperature dependence of the permittivity [127]. Thus an understanding of the factors that determine the dielectric behaviour of liquid crystals will help to develop the new materials having better display properties. Dielectric permittivities of nematic liquid crystals have extensively been studied both experimentally and theoretically [128-133].

2.5.1 MAIER AND MEIER THEORY OF DIELECTRICS FOR NEMATIC LIQUID CRYSTALS

Taking into account the polarization field in the medium W. Maier and G. Meier [134] extended the Onsager's theory [135] for isotropic dielectrics to nematics to correlate the dielectric properties with molecular parameters. According to Maier and Meier theory of nematics a molecule with polarizabilities $\alpha_{\parallel}$, $\alpha_{\perp}$ and permanent dipole moment μ having components $\mu_{\parallel} = \mu\cos\theta$, $\mu_{\perp} = \mu\sin\theta$, along and perpendicular to molecular long axis, is considered to be in a spherical cavity; θ is the angle between the molecular long axis and the dipole moment μ. The environment of this molecule is taken as a continuum with the macroscopic properties of the dielectric. The dielectric permittivities $\varepsilon_{\parallel}$ and $\varepsilon_{\perp}$ along and perpendicular to the molecular long axis are then given by

$$\varepsilon_{\parallel} = 1 + 4\pi NhF\left\{\bar{\alpha} + \frac{2}{3}\Delta\alpha S + F\frac{\langle\mu_{\parallel}^2\rangle}{kT}\right\} \qquad 2.29$$

$$\varepsilon_{\perp} = 1 + 4\pi NhF\left\{\bar{\alpha} - \frac{1}{3}\Delta\alpha S + F\frac{\langle\mu_{\perp}^2\rangle}{kT}\right\} \qquad 2.30$$

with

$$\langle \mu_{\parallel}^2 \rangle = \frac{\mu^2}{3}\left[1-(1-3\cos^2\theta)S\right]$$

$$\langle \mu_{\perp}^2 \rangle = \frac{\mu^2}{3}\left[1+\frac{1}{2}(1-3\cos^2\theta)S\right]$$

So that,

$$\Delta\varepsilon = \varepsilon_{\parallel} - \varepsilon_{\perp} = 4\pi NhF\left\{\Delta\alpha - F\frac{\mu^2}{2kT}(1-3\cos^2\theta)\right\}S \qquad 2.31$$

$$\bar{\varepsilon} = \frac{\varepsilon_{\parallel}+2\varepsilon_{\perp}}{3} = 1+4\pi NhF\left\{\bar{\alpha}+F\frac{\mu^2}{3kT}\right\} \qquad 2.32$$

Also, for isotropic state, when S=0, one gets the permittivity

$$\varepsilon_{iso} = 1+4\pi NhF\left\{\alpha_{iso}+F\frac{\mu^2}{3kT}\right\} \qquad 2.33$$

where N = the particle density = $\rho N_A/M$, ρ = mass density, N_A=Avogadro's number, M = Molecular weight, S= the order parameter and $\bar{\alpha}$= mean polarizability given by

$$\bar{\alpha} = \frac{\alpha_{\parallel}+2\alpha_{\perp}}{3} \qquad 2.34$$

$\Delta\alpha = \alpha_{\parallel} - \alpha_{\perp}$= polarizability anisotropy; h and F are respectively the cavity field factor and the reaction field factor and are given by

$$h = \frac{3\bar{\varepsilon}}{2\bar{\varepsilon}+1} \qquad \text{and} \qquad F = \frac{1}{(1-\bar{\alpha}f)}$$

Here, f, called Onsager factor, is given by

$$f = \frac{2N}{3\varepsilon_0}\frac{\bar{\varepsilon}-1}{2\bar{\varepsilon}+1}$$

The equations (2.29, 2.30) for $\varepsilon_{\parallel}$ and $\varepsilon_{\perp}$ are often used to compute the effective dipole moment of the molecules in nematic phase and its orientation with the molecular long axis.

Maier-Maier's equations satisfactorily explain many essential features of the permittivity of liquid crystals consisting of polar molecules. The experimental method for measuring static dielectric permittivities ($\varepsilon_{\parallel}$ and $\varepsilon_{\perp}$) will be discussed in section **2.7.3.**

2.6 FREQUENCY DOMAIN DIELECTRIC SPECTROSCOPY

DEBYE MODEL

In an ac field, because of the phase lag between the applied field and the displacement vector, dielectric permittivity (ε) become complex and for a dipolar liquid it is given by

$$\varepsilon^*(\omega) = \varepsilon'(\omega) - i\varepsilon''(\omega) = \varepsilon_\infty + \frac{\varepsilon_0 - \varepsilon_\infty}{1 + i\omega\tau} \qquad 2.35$$

This is known as Debye equation [136]. Here ε' and ε'' are respectively real and imaginary parts of complex dielectric permittivity, ε_0 is the static dielectric permittivity, ε_∞ is the high frequency limit of the dielectric permittivity and τ is the dielectric relaxation time.

One of the best methods to study dielectric behaviour of a material is to measure the complex dielectric permittivity as a function of frequency at constant temperature and ambient pressure. The frequency at which ε" reaches its maximum is known as critical frequency (or relaxation frequency). τ_c, the dielectric relaxation time related to the critical frequency (f_c) obtained from equation (2.35) is given by the relation:

$$\tau_c = \frac{1}{2\pi f_c} \qquad 2.36$$

The Debye equation (2.35) can be split into two separate formulae:

$$\varepsilon' = \varepsilon_\infty + \frac{\varepsilon_0 - \varepsilon_\infty}{1 + (\omega\tau)^2} \qquad 2.37$$

$$\varepsilon'' = \frac{\varepsilon_0 - \varepsilon_\infty}{1 + (\omega\tau)^2}\omega\tau \qquad 2.38$$

ε" reaches it's maximum at critical frequency:

$$\varepsilon''(f_c) = \varepsilon''_{max} = \frac{\varepsilon_0 - \varepsilon_\infty}{2} \qquad 2.39$$

where the difference $\varepsilon_0 - \varepsilon_\infty \equiv \Delta\varepsilon$ is the so called dielectric increment or dielectric strength.

If one plots both the components of the dielectric permittivity versus frequency on the logarithmic scale one obtain typical dielectric spectrum shown in **Figure 2.11.** Frequency dependence of ε' is known in the literature as the dispersion curve whereas that of ε" is called the absorption curve.

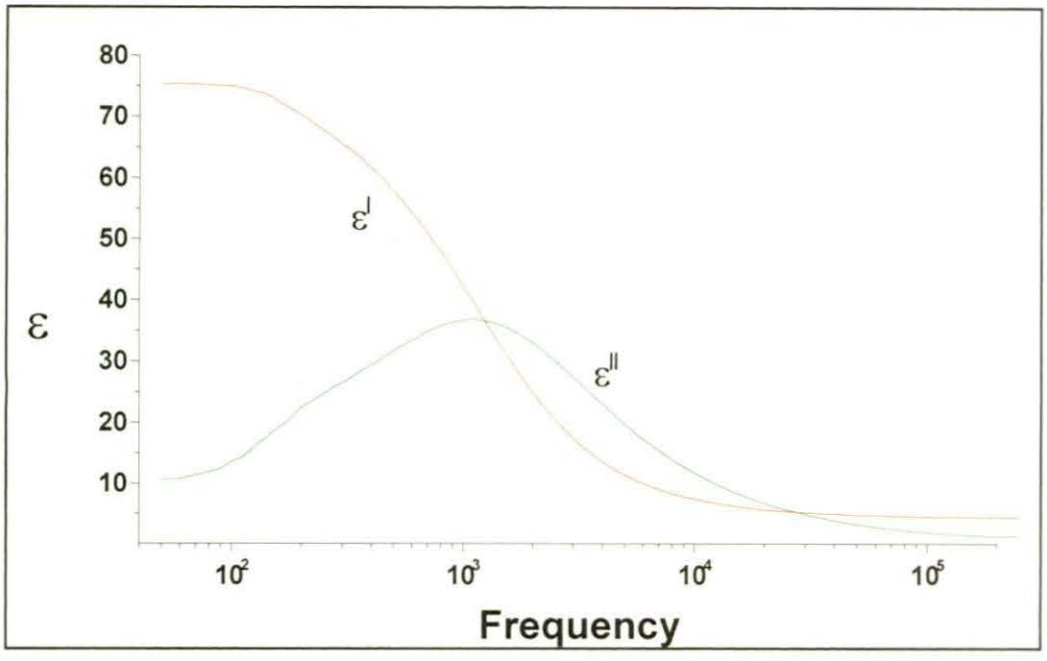

Figure 2.11. *A typical dielectric sprectra for a Debye type liquid crystal.*

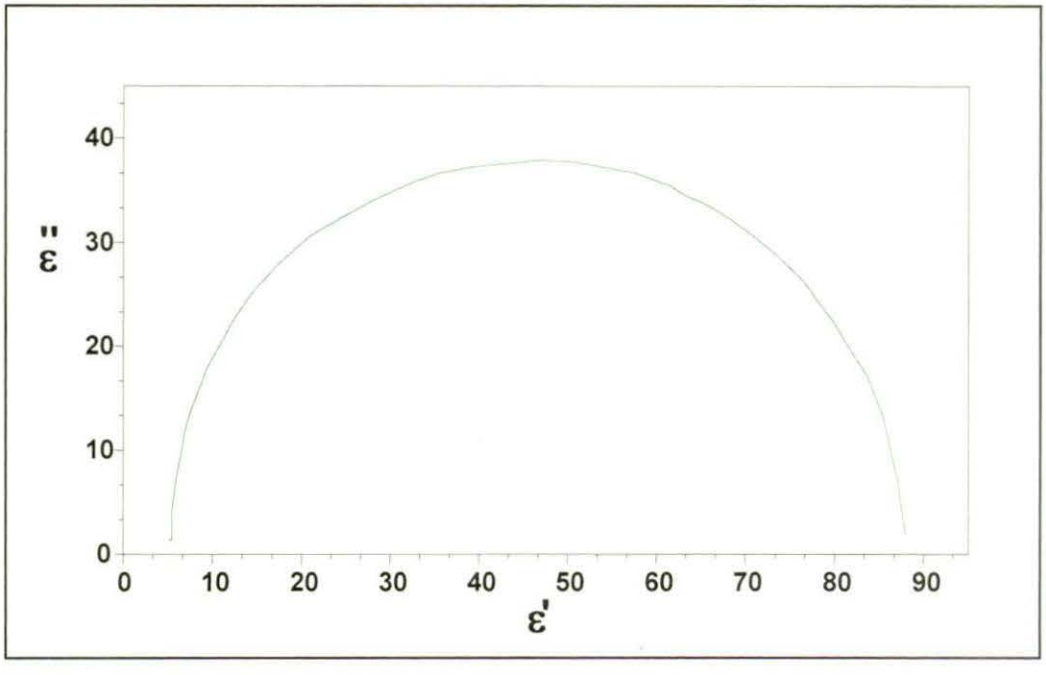

Figure 2.12. *Cole-Cole plot for a Debye-type spectrum.*

Dielectric spectra is also presented by plotting ε'' versus ε' on the complex plane which is known as Cole-Cole plot as shown in **Figure 2.12**. Each point (ε', ε'') on the Cole-Cole plot represents complex dielectric permittivity obtained at a certain frequency. One should add that for the Debye-type process the Cole-Cole plot is a semicircle with the center lying on the ε' axis at $(\varepsilon_0 + \varepsilon_\infty)/2$ with $\frac{\varepsilon_0 - \varepsilon_\infty}{2}$ as radius.

COLE-COLE MODEL

Dielectric spectroscopy in nematics and in para-, ferro-, ferri- and antiferro-electric liquid crystals [136], gives idea about reorientation of molecular dipole moments and collective fluctuations of spontaneous polarization governed by the law of probability. For liquids and solid rotator phases of organic polar compounds [137,138] the dielectric spectrum is usually of a Debye-type. However, some systems composed of flexible molecules [138-141] and some disordered solid phases [142-144] exhibit broad dielectric spectra and can be described [138,142,145] by the Cole-Cole function [146]:

$$\varepsilon^* = \varepsilon' - i\varepsilon'' = \varepsilon_\infty + \frac{\varepsilon_0 - \varepsilon_\infty}{1 + (i\omega\tau_0)^{1-\alpha}} - i\frac{\sigma}{\omega\varepsilon_0} \qquad 2.40$$

which can be separated into two components:

$$\varepsilon'(\omega) = \varepsilon_\infty + \Delta\varepsilon \frac{1 + (\omega\tau_0)^{1-\alpha} \sin\left(\frac{1}{2}\pi\alpha\right)}{1 + 2(\omega\tau_0)^{1-\alpha} \sin\left(\frac{1}{2}\pi\alpha\right) + (\omega\tau_0)^{2(1-\alpha)}} \qquad 2.41$$

$$\varepsilon''(\omega) = \Delta\varepsilon \frac{(\omega\tau_0)^{1-\alpha} \cos\left(\frac{1}{2}\pi\alpha\right)}{1 + 2(\omega\tau_0)^{1-\alpha} \sin\left(\frac{1}{2}\pi\alpha\right) + (\omega\tau_0)^{2(1-\alpha)}} + \frac{\sigma}{\omega\varepsilon_0} \qquad 2.42$$

where $\Delta\varepsilon = \varepsilon_0 - \varepsilon_\infty$ is the dielectric strength, α is a parameter responsible for symmetric distribution of the relaxation times and τ_0 is in this case the most probable relaxation time related to the critical frequency ($\omega_0\tau_0=1$). $\varepsilon_0 = 8.85$ pFm^{-1} is the dielectric permittivity of the free space and σ is the conductivity. Here conductivity related to the motion of charge carriers is added to classical Cole-Cole function. The maximum value of $\varepsilon''(\omega)$ depends on the parameter α according to the formula:

$$\varepsilon''(\omega_c) = \varepsilon''_{max} = \frac{\varepsilon_0 - \varepsilon_\infty}{2} \frac{\cos\frac{\pi\alpha}{2}}{1 + \sin\frac{\pi\alpha}{2}} \qquad 2.43$$

For small values of the α parameter ($\alpha < 0.1$) one can use the formula:

$$\varepsilon''_{max} \cong \frac{\varepsilon_0 - \varepsilon_\infty}{2 + \alpha\pi} \qquad 2.44$$

From the above formula it is seen that for non-Debye dielectric relaxation processes the absorption peak is lower and broader as shown in **Figure 2.13**. A more general function was proposed by Havriliak and Negami [147,148]. Relaxation processes that could be described by this kind of function were observed for polymers, some disordered solids and also FLCs as well as AFLCs [149-156].

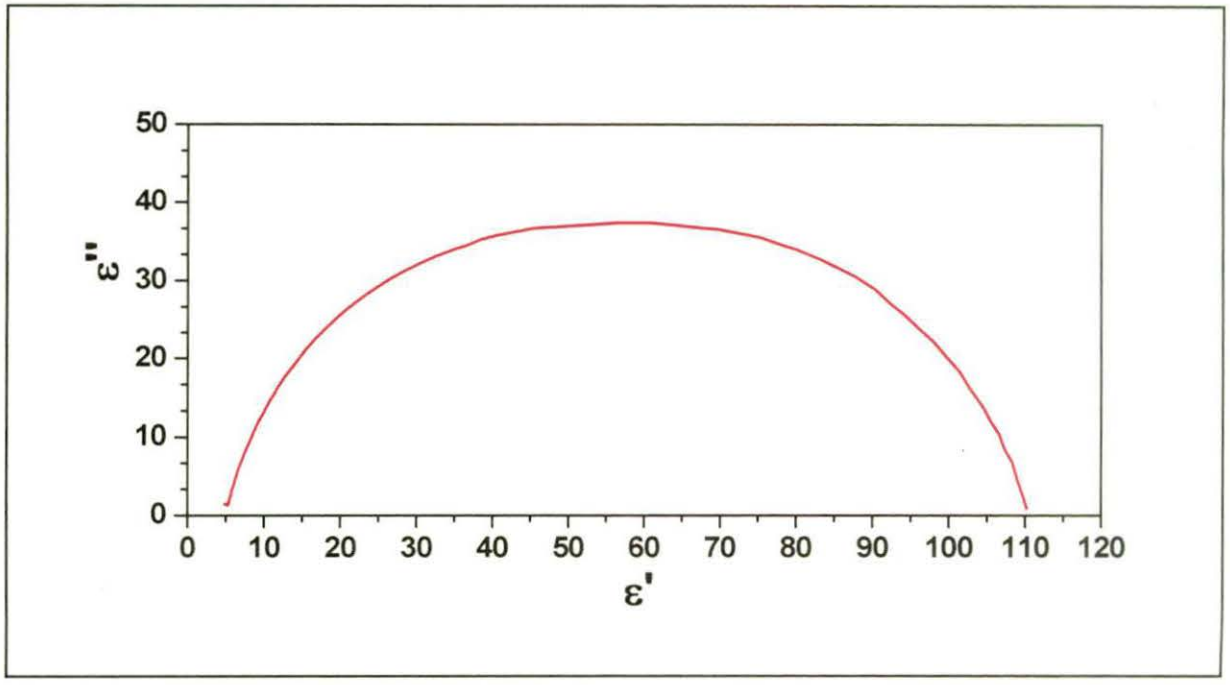

Figure 2.13. *Cole-Cole plot for a Cole-Cole type spectrum*

2.7 DIFFERENT RELAXATION PROCESSES IN CHIRAL AND ACHIRAL LIQUID CRYSTAL PHASES

There are several relaxation processes in chiral and achiral liquid crystal phases. Both types of molecular processes; collective and non-collective (single molecular) exist in chiral and achiral phases.

2.7.1 NON-COLLECTIVE PROCESS

When an achiral low molecular mass nematic liquid crystal is subjected to an ac field two non-collective molecular mode dielectric relaxations are observed. One is associated with rotation of the molecules around its short axis, the other occurs when the molecule rotates around its long axis. Other than positional ordering, reorientations of entire molecules around their short and long axes are one of the features that distinguish the liquid crystalline state.

In order to discuss the relaxation processes in the dielectric spectrum of the nematic phase [157], let us consider a molecule with a permanent dipole moment which makes an angle β with the long axis of a molecule shown in **Figure 2.14.** For nematic liquid crystal the order parameter always less than one, therefore each of the components of dipole moment, longitudinal and transverse to the long axis (μ_l and μ_t), should have a non zero projection both parallel and perpendicular to the director **n**, resulting in four relaxations, two in each measurement geometry, **E**||**n** and **E**⊥**n**.

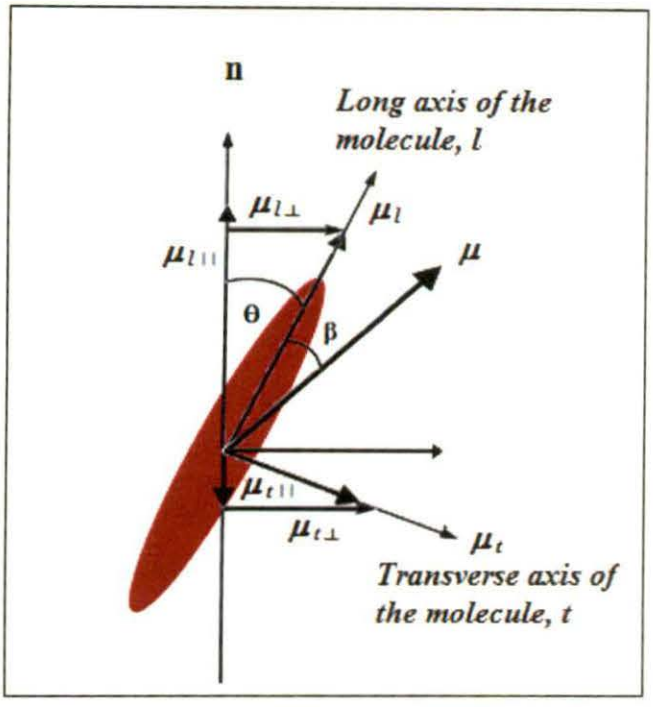

Figure 2.14. *The molecular aspect of different dielectric absorption peaks.*

But because of weak intensities of two absorptions related to μ_l and μ_t, we are left with two fundamental and characteristic absorptions of non-collective types in the chiral and achiral liquid crystal phases: one absorption is observed in the homeotropic orientation, which is assigned to the molecular reorientation around the short axis of molecule. This molecular rotation is hindered by the nematic potential, hence shifted to the low MHz and kHz region from the GHz and high MHz regime observed in normal liquids,. The second absorption is observed in the planar orientation, which is assigned to the molecular rotation around the long axis of molecule. The molecular rotation is not affected by the nematic potential; therefore its characteristic frequency is observed in the high MHz and GHz regime.

2.7.2. COLLECTIVE PROCESSES

Besides the non-collective processes, the dielectric spectrum of the chiral smectic liquid crystals contains two additional collective processes connected with the director fluctuation. In the SmA* phase, there exists one process assigned to the tilt fluctuation of the director and known as the soft mode. The mechanism is usually observed in the kHz regime with strong temperature dependence. In the SmC* phase, beside director tilt fluctuations it is subjected to huge phase fluctuations; in other words the molecules collectively oscillate around the smectic cone in a way roughly similar to the motion of a snake rolling itself on long tree; this mode is called the Goldstone mode [157]. This process has a characteristic frequency which varies in the Hz to kHz region with weak temperature dependence. It is to be mentioned here that these two modes are thermally activated.

2.7.2.1 GOLDSTONE MODE AND SOFT MODE

The Goldstone mode (GM) and the soft mode (SM), can be examined by dielectric relaxation spectroscopy [158-161]. The Goldstone mode, as stated before, appears in the SmC* phase because of the phase fluctuations in the azimuthal orientation of the directors. The soft mode appears due to the fluctuations of the tilt angle of the molecular directors at much higher frequency, in the vicinity of the SmA^*- SmC^* transition point. The GM dielectric increment ($\Delta\varepsilon_G$) is usually large compared to the SM increment ($\Delta\varepsilon_S$), so it is difficult to study the SM mode properties in the SmC^* phase. Yet, this problem can be overcome by applying a DC bias field to the SmC^* phase, the field should be strong enough to unwind the helical arrangement of the polarization vector. The SM can be studied almost separately by suppressing GM in this situation. Although GM dielectric increment is usually large compared to the SM increment but SM critical frequency is at least two order higher than that of GM. Moreover, according to the generalized Landau model [162] GM critical frequency remains almost independent of temperature whereas that of SM is strongly temperature dependent being associated with the tilt fluctuation of the directors.

From Landau model concept of soft mode was first introduced to the SmA*-SmC* phase transition by Blinc and Zeks [163] for the case of a modulated structure and later modified by Carlsson *et al.* [162] where phase transition is described in terms of two order parameters – two-component tilt vector as primary order parameter and two-component in-plane polarization as the secondary order parameter. Two characteristics modes are observed in SmA*-SmC* second order phase transition where the continuous symmetry group of SmA*

(D_∞) is spontaneously broken in SmC*(C_2). Whereas the soft mode is a symmetry breaking mode, which critically slows down (softens) on approaching the phase transition from above, the Goldstone mode is zero frequency mode that tries to restore the broken symmetry. Thus soft mode splits into the phase (GM) and amplitude (SM) modes in SmC* near the transition.

2.7.3 DIELECTRIC MEASUREMENTS

Dielectric measurements were made using an impedance analyzer (**HP 4192A / HIOKI 3532-50**) equipped with data acquisition system through **RS232** interface as shown in **Figure 2.15**. The temperature was measured with the help of a thermocouple inserted in the sample holder block and regulated with accuracy of ±0.1°C by a Eurotherm temperature controller

Figure 2.15. *Experimental set up of the dielectric spectrometer.*

(2216e). The dielectric spectra were measured over the frequency range from 40 Hz to 5 MHz or 10 Hz to 13 MHz. Commercial cells (EHC/AWAT), of thickness few μm, were used in the form of a parallel plate capacitors made of indium tin oxide (ITO) coated glass plates which were pre-rubbed by polymer for achieving homogeneous (HG) alignment of the molecules. By applying sufficient DC bias field homeotropic (HT) alignment of the molecules were achieved in the same cell. HG cell gives the $\varepsilon_\perp$ component when the measuring electric field was perpendicular to the nematic director and HT cell gives the $\varepsilon_\parallel$ component, measuring field being parallel to the director as shown **in Figure 2.16**. On the other hand, custom built gold cells of thickness few μm and effective area 1.3 x 0.7 sq. cm were used for frequency

dependent complex dielectric permittivity measurements. To see the effect of cell thickness and alignment layers, relaxation behaviour was also studied using ITO coated cells, pre-treated with polyimide for homogeneous and homeotropic alignment.

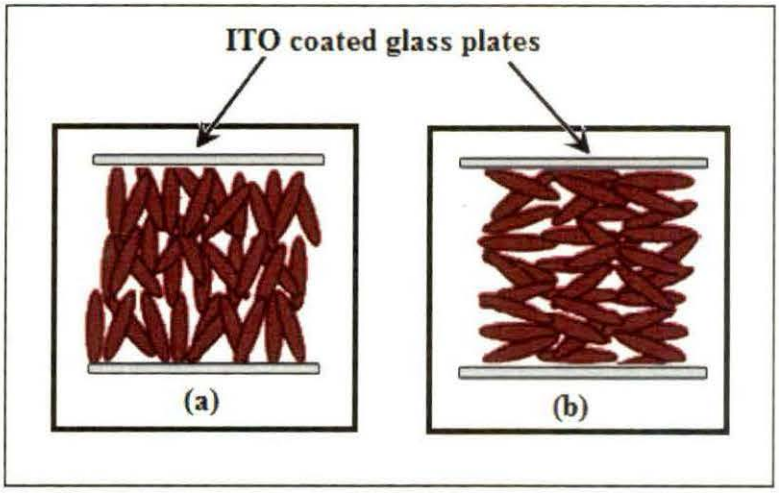

***Figure 2.16(a)**. Homeotropic and (**b**) Homogeneous alignment of liquid crystals.*

2.8 SPONTANEOUS POLARIZATION (P_S)

Unlike solid ferroelectrics, polarization is the secondary order parameter in FLCs. From the application point of view, the response time or switching time (τ) of an FLC device is the most significant parameter and is given by [70]

$$\tau = \frac{\gamma \sin\theta}{P_S E} \qquad 2.45$$

where γ is rotational viscosity, θ is tilt angle and E is the applied electric field. Thus to achieve faster switching speed τ should be as low as possible. For a portable device of low power consumption applied field E should be low. Therefore, viscosity γ and tilt angle θ should be low and P_s should be high. But a high value of P_S causes a current flow through the cell, which is undesirable. So a moderate level of P_S is required for a short switching time.

There are number of methods to measure the magnitude of P_s. Three widely used methods for determining P_s are (i) Sawyer-Tower method [165], (ii) reversal current method using a triangular wave[166]. (iii) reverse field method[167]. Here, the reversal current method using a triangular wave is explained since it has some unique advantages - use of this waveform separates the capacitive contribution from interfering with current due to polarization reversal. Experimental set up for reversal current method using a triangular wave

is shown in **Figure 2.17**. Liquid crystalline compounds are not insulators. Hence, a liquid crystal cell can be regarded as a resistor 'R' and a capacitor 'C' connected in parallel. The current I(t) induced in a ferroelectric liquid crystal cell by applying a potential V(t) is written as a sum of the following three contributions [168]: (i) displacement current I_c due to charge accumulation in the capacitor, (ii) the polarization realignment current I_p and (iii) ionic flow current I_i.

$$I = I_C + I_P + I_i = C\left(\frac{dV}{dt}\right) + \frac{dP}{dt} + \frac{V}{R} \qquad 2.46$$

where P is the amount of charge induced by the polarization reversal in the cell on application of an electric field. **Figure 2.18** shows the contribution of three components to the overall current response.

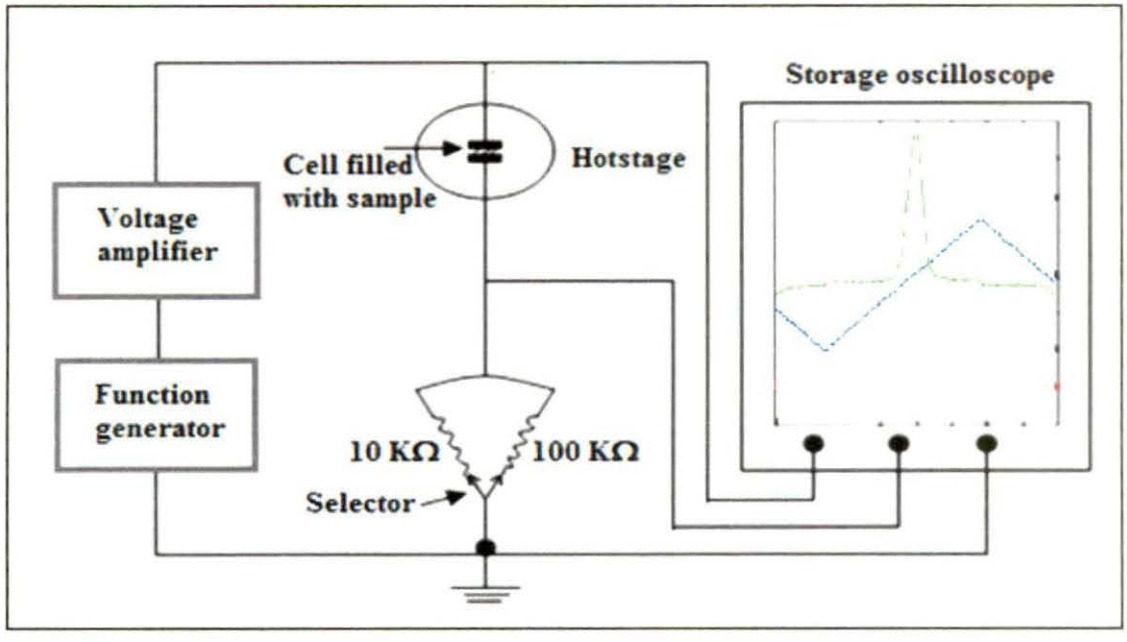

Figure 2.17. *Experimental set up to measure the value of P_s*

In this measurement, current signal has been converted to voltage signal through a resistor(R). Since the time constant of the circuit is small, the current due to the charge accumulation is well resolved from the current peak due to the polarization reversal. When P_s is small, a large resistor or an amplifier must be used. In the reversal current method, however, the contribution of Ic and I_i appears as a straight line. In this respect, the subtraction of the base line is easier in this method.

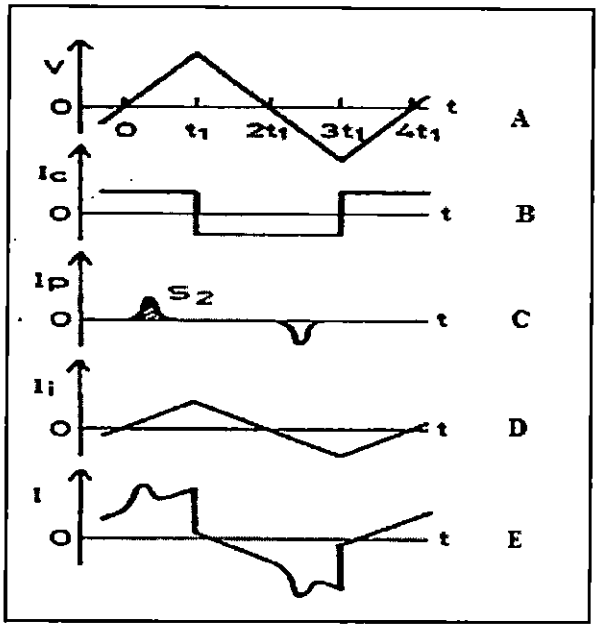

Figure 2.18. Schematic illustration of the reversal current method using a triangular wave to FLC, (A) applied triangular wave, (B) contribution due to charge accumulation I_c, (C) polarization realignment current I_p,(D) ionic current I_i, (E) overall current profile.

10 Hz, 20Vpp signal was used from **HP 34401A** function generator, amplified by **F20A** Voltage amplifier. **HP 500** MHz Infinium/ **Tektronix TDS 2012B** storage oscilloscope was used to record the voltage drop. One has to be careful when the material is relatively conductive and an applied electric field of low frequency is used. Ionic flow possibly gives rise to a current peak, which is sometimes reminiscent to the switching current peak.

The area under the polarization current peaks gives direct estimate of P_s

$$Ps = \frac{\int Vdt}{2AR} \qquad 2.47$$

where, R is the resistance used to record the V-t curve and A is the effective area of the sample used. Area under the curve was determined from the stored image after creating appropriate base line using Microcal Origin software.

2.9 CRYSTAL STRUCTURE DETERMINATION

The gathering knowledge of the structure of both molecular and non-molecular materials is one of the fundamental aims of scientists. The term 'structure' has many meanings; here it is to be the relative positions of the atoms or ions which make up the substance under study and hence a geometrical description in terms of bond lengths and angles, torsion angles, non-bonded distances and other quantities of interest. This knowledge makes possible the pictorial representation of chemical structures of the liquid crystalline molecule. The knowledge of the molecular structure in the crystalline state is very helpful for proper understanding and interpretation of several physical properties of liquid crystals. The molecular conformation in the crystalline state predetermines the molecular organization in the mesomorphic state. Bernal and Crowfoot [169] in the early 1930's, made the first attempt to correlate the molecular arrangement in the mesomorphic state with the crystal structure of the mesogenic material. However, after that a very few studies had been done for many years in the crystal structure determination. In the late 70's, due to the introduction of computer programs for solving structures a large number of structures of liquid crystal forming compounds have been determined which are mostly nematogens [170-184]. Introductory investigation on the present information of the structure-property relationship is given by Bryan [185] and later by Haase and Athanassopoulou [186]. Crystal structures of a number of mesogenic compounds had also been reported from our laboratory in order to investigate the structure-property relationship [170-178]. From available results it can be stated, in general, that

(i) the molecules of the liquid crystalline compounds on heating adopt an arrangement some what similar to that in the crystals.

(ii) the long and narrow molecules are more or less parallel and interleave one another to form an 'imbricated packing' in a nematogenic crystal.

(iii) the molecules are found to be packed in parallel layers in a smectogenic crystal.

Though in large number of known cases the above features are true, but for the generalization precaution must be made since examples are also known where it is not true [186,187].

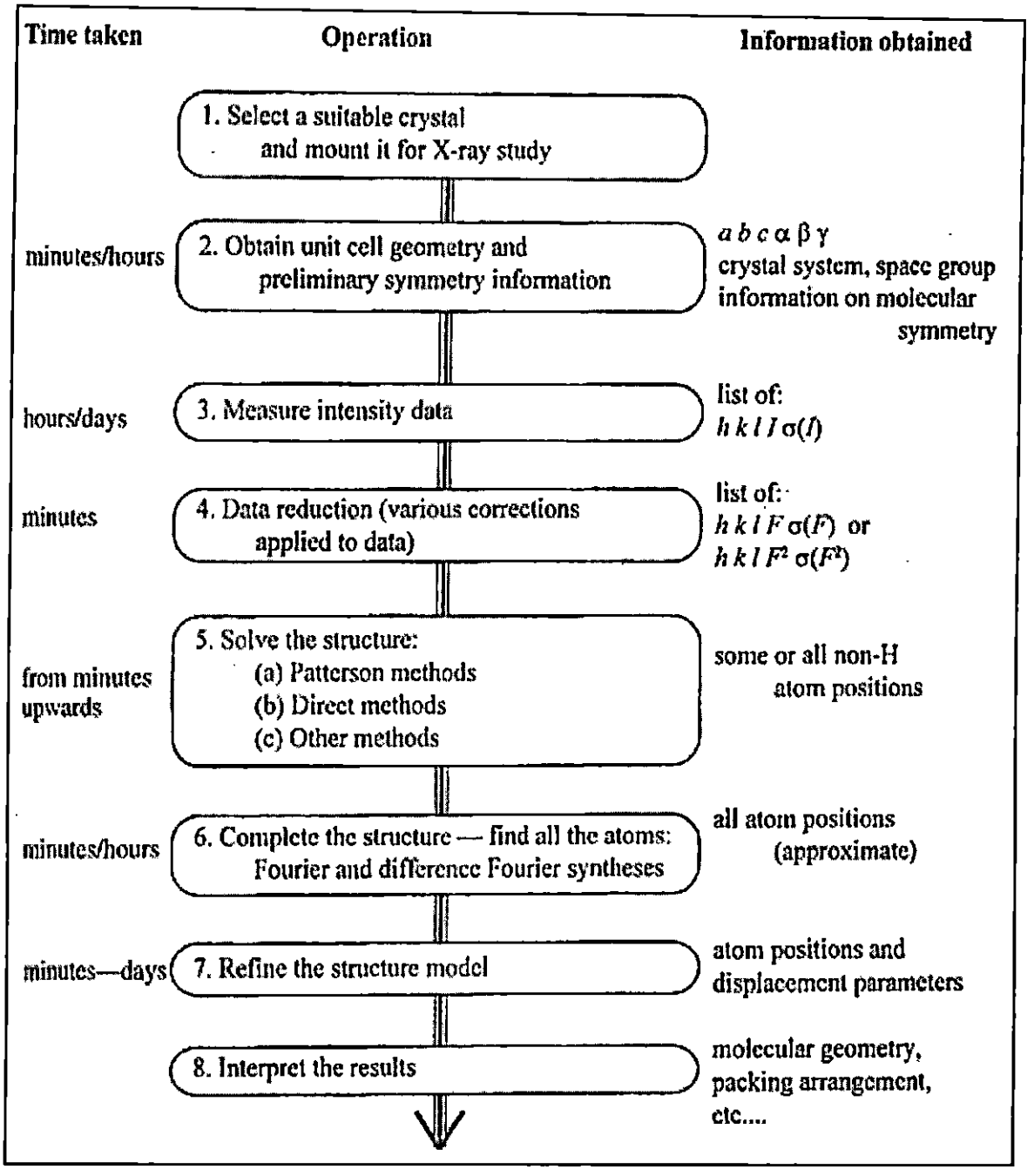

Figure 2.19. flowchart for the steps involved in a crystal structure determination

The schematic flow chart (Figure 2.19) shows the outline of crystal structure determination in a simplified form [188]. The steps involved are shown in boxes. To the right of each is listed the information obtained and to the left an indication of the time-scale involved in carrying out the operation. Some of these times vary considerably, depending on the quality of the sample being studied, the sources available for the work, the size and complexity of the structure and the skill of the crystallographer.

2.9.1 THEORY OF CRYSTAL STRUCTURE DETERMINATION

In a crystal the constituent atoms or molecules are arranged in a regular and periodic manner with long range positional and orientational order. One can build a unit cell, with edges given by three non coplanar vectors **a, b, c** and the angles α, β, γ between the edges. Both photographically and with a diffractometer the unit cell geometry can be measured from a subset of the complete diffraction pattern. The key step is assigning the correct indices hkl to each of the observed reflections. From these and the measured Bragg angle for a few reflections, the six unit cell parameters can be calculated via the Bragg equation and modified versions of it appropriate to the geometry of the particular camera or diffractometer being used. In CAD4 diffratometer collection of intensity data are controlled by a computer.

To locate the positions of the individual atoms in the unit cell, the intensity of the diffracted pattern must be measured and analysed. If f_j be the amplitude scattered by the j-th atom at point $\mathbf{r}_j$ and if there are N such atoms within the cell, then the amplitude of the radiation scattered from the array of planes represented by the Miller indices (hkl) is given by [189],

$$F_{hkl} = \sum_{j=1}^{N} f_j \exp 2\pi i(hx_j + ky_j + lz_j) \qquad 2.48$$

The quantity f_j is called atomic scattering factor or form factor, F_{hkl} is known as the structure factor for the reflection hkl. $|F_{hkl}|$ is called the structure amplitude, is a pure number- number of electrons. The above equation may also be written as

$$F_{\mathbf{H}} = \sum_{j=1}^{N} f_j \exp\left(2\pi i \mathbf{H}.\mathbf{r}_j\right) \qquad 2.49$$

Where the reciprocal lattice vector has been replaced by **H**

As the atoms in the unit cell are at the positions of high electron density $\rho(\mathbf{r})$, so $F_{\mathbf{H}}$ can be expressed as

$$F_{\mathrm{H}} = \int_V \rho(\mathrm{r}) \exp\left(2\pi i \mathbf{H}.\mathbf{r}\right) dV \qquad 2.50$$

where V is the volume of the unit cell. Since $\rho(\mathbf{r})$ is periodic in three dimensions, by Fourier transformation we have

$$\rho(\mathbf{r}) = \frac{1}{V} \sum_h \sum_k \sum_l F_{\mathbf{H}} \exp(-2\pi i \mathbf{H}.\mathbf{r}) \qquad 2.51$$

From a large number of F_H obtained by diffraction experiment, one could have directly derived the crystal structure by Fourier summation. However, from diffraction experiments one gets a set of diffracted intensities (I_H) from different hkl planes. From these values we can get the magnitude of the structure factors $|F_H|$, but not their phases ϕ_H and this constitutes the phase problem in crystallography. To overcome phase problem, four main methods, (i) *Patterson method*, (ii) ***Direct methods***, (iii) *Isomorphous replacement technique* and (iv) *Anomalous scattering method* - are available. Only ***direct methods*** [190] will be discussed here, because the structures of liquid crystalline forming compound have been determined by this method.

DIRECT METHODS

This is a general name given to methods which seek to obtain approximate phases ϕ_H directly from the measured intensities (I_{obs}) by probabilistic calculations. Direct methods involve selecting the most important reflections (those which contribute most to the Fourier transform), working out the probable relationships among their phases, then trying different possible phases to see how well the probability relationships are satisfied. For the most promising combinations (assessed by various numerical measures), Fourier transforms are calculated from the observed amplitudes and trial phases and are examined for recognizable molecular features. The direct methods are very efficient in solving crystal structures especially of low molecular weight organic compounds following the work of Herbert Hauptman and Jerome Karle for which they were awarded Novel prize in chemistry in 1985.

Now several computer programs are available for determining crystal structures by direct methods viz., MULTAN[191], SHELX [192], XTAL [193], SAPI [194], SIR[195], NRCVAX [196], MITHRIL[197], DIRDIF [198] etc. Many books and monographs [189, 190 199-202] are available where details of the above methods have been described.

A systematic account of the development of the direct methods is beyond the scope of this thesis. Only the basic principles and working formulae will be discussed here.

STRUCTURE INVARIANTS AND SEMINVARIANTS

One of the recurring difficulties in solving the phase problem involves defining the origin of the unit cell properly with respect to the symmetry elements and all the contents of the cell. Shifting the origin arbitrarily does not affect the structure amplitudes ($|F_{hkl}|$) but may change the phases (ϕ_H) drastically. Consequently, the selection of phases intimately associated with the choice of origin. There exists, however, certain combinations of phases

that do not vary regardless of the arbitrary assignment of cell origin. Therefore, a structure invariant is defined as a quantity that is independent of the shift of the origin of the unit cell.

The intensities I_H of reflections i.e. $|F_H|^2$ are structure invariants. However the structure factor itself is not structure invariant, otherwise the phase problem would not occur. This is because, for any shift in the origin by, say, $\Delta\mathbf{r}$ the phase of F_H changes by - $2\pi\mathbf{H}.\Delta\mathbf{r}$ radians while the amplitude remains invariant. Similarly it can be shown that $|F_H|^2$ is structure invariant. Though individual phases depend on the structure and choice of origin, some combinations of them is structure invariant. For example, if $\mathbf{H_1}+\mathbf{H_2}+\mathbf{H_3}=0$ then $\phi_{H_1} + \phi_{H_2} + \phi_{H_3}$ is structure invariant for every space group. It follows directly from the fact that the product $F_{-H}F_KF_{H-K}$ is an invariant. Since the moduli of the structure factors are invariant themselves, the angular part of $F_{-H}F_KF_{H-K}$ is also invariant i.e. $\phi_{-H} + \phi_K + \phi_{H-K} = \phi(\mathbf{H},\mathbf{K}) = \phi_3$ is invariant.

The structure seminvariants are quantities that do not change value on transfer from one permissible origin of a space group to another. The structure seminvariants are those linear combinations of the phases whose values are uniquely determined by the crystal structure alone, when the choice of origin is restricted within permissible values. It originates from space group symmetry. For example in space group P $\bar{1}$, the linear combination $2\phi_{-H} + \phi_{2H}$ is a structure invariant for any reciprocal vector **H.** For each space group they have to be derived separately. In any space group any structure invariant is also a structure seminvariant, but reverse is always not true. A complete theory is given in a series of papers by Hauptman and Karle [203-205] and by Schenk [201].

2.9.2 PROCEDURES FOR STRUCTURE DETERMINATION

Single crystals are grown from a solution usually by a slow evaporation technique. Quality of single crystals are tested under polarizing microscope and crystals of suitable dimensions are used for data collection. Usually using CuK_α/MoK_α radiation, the intensity data are collected from the single crystal by computer-controlled CAD4 X-ray diffractometer. The intensity data are corrected for Lorentz polarization factors [189]. The intensities are converted into the structure factors on an absolute scale by determining the scale factor by the method introduced by A. J. C Wilson [206]. The temperature factors are also found to take into account the thermal vibrations of the atoms during the process. Then the following steps are taken:

1st. Estimation of normalised structure factors |E|'s from $|F_{obs}|$ values

2nd. Set up of phase relationships via structure invariants and seminvariants, starting phase determination, phase extension and refinement

3rd. Calculation of figures of merit of different phase sets

4th. Production of E-map by Fourier method and their interpretation to get the trial structure consistent with the molecular structure

5th. Refinement of structures through Fourier synthesis, difference Fourier synthesis and least-square refinement techniques.

ESTIMATION OF |E|'S FROM $|F_{OBS}|$ VALUES

The phases of the structure factors in direct methods are estimated directly from the structure amplitudes so the decrease of the atomic scattering factor with increasing scattering angle has to be eliminated. The observed $|F_H|$ is therefore modified so that they correspond to the hypothetical diffracted waves which would be obtained if atoms were stationary point atoms at rest [201]. Normalized structure factors, E_H, are related to F_H in the following way:

$$|E_H|^2 = \frac{I_h}{\langle I \rangle} = \frac{|F_H|^2}{\varepsilon \sum_{j=1}^{N} f_j^2} \qquad 2.52$$

and $\langle |E_H|^2 \rangle = 1$

The factor ε simply takes care of the degeneracy of an F_H if it lies on a symmetry location in the reciprocal structure. Naturally the sign of E_H is the same as that of the corresponding F_H.

TRIPLET PHASE RELATIONSHIPS, STARTING PHASE DETERMINATION, PHASE EXTENSION AND REFINEMENT

The practical objective of direct method is to phase a sufficient number of reflections to give an identifiable Fourier representation of the molecule being studied. The number required will depend on various factors, among them the nature of the molecular system and how much is already known of its structure are important. Initially phases of only the strongest reflections are determined. Roughly, however, 10 reflections per atom in the asymmetric unit seem quite satisfactory and in some cases as few as three to five per atom have served.

The most commonly used phase relation is a three phase structure invariants based on the positivity of electron density criterion, as proposed by Hauptman and Karle [203, 204]:

$$\phi_{\mathbf{H}} \approx \phi_{\mathbf{K}} + \phi_{\mathbf{H}-\mathbf{K}} \qquad 2.53$$

For centrosymmetrical crystals the sign relation is expressed as

$$S(\mathbf{H}) \approx S(\mathbf{K})\, S(\mathbf{H}-\mathbf{K}) \qquad 2.54$$

Relation (2.53) is used to generate phases $\phi_{\mathbf{H}}$ when the values of the phases on the right-hand side are known and it is used in a cyclic manner to propagate the phases to all the selected reflections. These relations are probability relations and the probability is high when the reflections have large |E| values in addition to satisfying the criterion $\mathbf{H} + \mathbf{K} + \mathbf{L} = 0$. These are called triplet or Σ_2 phase relations. Probability of the phase of **H** being equal to the sum of the phases of **–H** and **H-K** is given by the following relations. In centrosymmetric case [207]:

$$P_{+}(\mathbf{H},\mathbf{K}) = \frac{1}{2} + \frac{1}{2}\tanh\left[\frac{1}{2}k(\mathbf{H},\mathbf{K})\right] \qquad 2.55$$

here $$k(\mathbf{H},\mathbf{K}) = 2\sigma_3\sigma_2^{-\frac{3}{2}}|E_{\mathbf{H}}||E_{\mathbf{K}}||E_{\mathbf{H}-\mathbf{K}}|$$

$$\sigma_n = \sum_{j=1}^{N} Z_j^n$$

Z_j being the atomic number of the j^{th} atom in a unit cell containing a total of N atoms. For identical atoms $\sigma_3\sigma_2^{-\frac{3}{2}} = N^{-\frac{1}{2}}$.

In non-centrosymmetric case [208]:

$$P[\phi(\mathbf{H},\mathbf{K})] = \frac{\exp\{k(\mathbf{H},\mathbf{K})\cos[\phi(\mathbf{H},\mathbf{K})]\}}{2\pi I_o\{k(\mathbf{H},\mathbf{K})\}} \qquad 2.56$$

where I_o is a zero-order modified Bessel function of the first kind.

Now the question arises about deciding the phase of a particular reflection when there are several pairs of known phases, the estimate from each of which might be well different. The answer to this important problem was given by Karle and Hauptman [209] in 1956. They introduced the tangent formula

$$\tan\phi_{\mathbf{H}} \approx \frac{\sum_{\mathbf{K}} k(\mathbf{H},\mathbf{K})\sin\left(\phi_{\mathbf{K}} + \phi_{\mathbf{H}-\mathbf{K}}\right)}{\sum_{\mathbf{K}} k(\mathbf{H},\mathbf{K})\cos\left(\phi_{\mathbf{K}} + \phi_{\mathbf{H}-\mathbf{K}}\right)} = \frac{B(\mathbf{H})}{A(\mathbf{H})} \qquad 2.57$$

In order to use the tangent formula to obtain a new phase, the value of some phases have to be known and put into the right -hand side of the tangent formula. The set of the known phases is called a starting set from which the tangent formula derives more and more new phases and refines them in a self-consistent manner. But in this way all phases cannot be determined with acceptable reliability. It is therefore useful at this stage to eliminate about 10% of these reflections whose phases are most poorly defined by the tangent formula (2.57). An estimate of the reliability of each phase is obtained from $\alpha(\mathbf{H})$:

$$\alpha(\mathbf{H}) = \left\{A(\mathbf{H})^2 + B(\mathbf{H})^2\right\}^{\frac{1}{2}} \qquad 2.58$$

when the relation (2.58) contains only one term, as it may in the initial stages of the phase determination, then $\alpha(\mathbf{H}) = k(\mathbf{H},\mathbf{K})$.

The larger the value of $\alpha(\mathbf{H})$, the more the reliable is the phase estimate. The relation between $\alpha(\mathbf{H})$ and the variance is given by Karle and Karle [205], in 1966, as

$$\sigma^2(\mathbf{H}) = \frac{\pi^2}{3} + 4\sum_{t=1}^{\infty} \frac{(-1)^t I_t\{\alpha(\mathbf{H})\}}{t^2 \; I_0\{\alpha(\mathbf{H})\}} \qquad 2.59$$

From (2.58) it can be seen that $\alpha(\mathbf{H})$ can only be calculated when the phases are known. However, an estimate of $\alpha(\mathbf{H})$ can be obtained from the known distribution of three phase structure invariants [207]. The estimated $\alpha(\mathbf{H})$ at the initial stage is given approximately by

$$\alpha_{est}(\mathbf{H}) = \sum_{\mathbf{K}} k(\mathbf{H},\mathbf{K}) \frac{I_1\{k(\mathbf{H},\mathbf{K})\}}{I_0\{k(\mathbf{H},\mathbf{K})\}} \qquad 2.60$$

As the tangent phasing process is usually initiated with a few 'known' phases so to fix the origin and enantiomorphs is the first step in phase extension. This is done imposing the condition in terms of structure factor seminvariant phases. The selection of starting phases is critical to the success of the multisolution methods. The generator reflections are sorted by a convergence-type process by Germain, Main and Woolfson [210] which maximises the connection between starting phases. At the end of the convergence procedure a number of reflections, sufficient to fix the origin and the enantiomorphs whose phases are known, are obtained. A few other reflections are also chosen to which different phase values are assigned (either numerically or symbolically) to create different starting points for phase extension through Σ_2 relations. The strength of convergence procedure is that it ensures, as far as possible, that the initial phases will develop through strong and reliable phase relationships. For each starting phase set, phases of all the selected strong reflections are generated and refined as explained in earlier section. Thus we get a multiple phase sets.

CALCULATION OF FIGURE OF MERIT OF THE GENERATED PHASE SETS

When a number of sets of phases have been developed, it is necessary to rank them according to some Figure-of-Merit (FOM), prior to computing a Fourier map (in this case E-map). Combining all weights from various FOM viz., Absolute Figure-of-Merit (ABSFOM), Relative Figure-of-Merit (RFOM), R-factor Figure-of-Merit (RFAC), Psi (zero) Figure-of-Merit (PSIO) etc. Combined Figure-of-Merit (CFOM) are calculated for each set. The most likely correct sets of phases are those with the highest value of CFOMs [211].

E-MAP CALCULATION AND INTERPRETATION

Using the best phase set, E-maps are calculated using equation (2.51) at a large number of grid points covering the entire unit cell. The complete interpretation of the maps is done in three stages: peak search, separation of peaks into potentially bonded clusters and application of simple stereochemical criteria to identify possible molecular fragments. The molecular fragments thus obtained can be compared with the expected molecular structure. The computer can thus present the user with a list of peaks and their interpretation in terms of the expected molecular structure quite automatically. It is also common practice to have an output of the picture of the molecule as an easy check on the structure the computer has found.

REFINEMENT OF STRUCTURES THROUGH FOURIER SYNTHESIS, DIFFERENCE FOURIER SYNTHESIS AND LEAST- SQUARE REFINEMENT TECHNIQUE

Generally for refinement of a model structure (partial or complete) obtained from E-map three methods are used [189, 200] e.g., 1) Fourier synthesis, (2) Difference Fourier synthesis and (3) Least squares refinement.

The Fourier synthesis gives the refined co-ordinates of the atoms and also tends to reveal the position of any atom that is not included in computing the structure factors using equation (2.48). The difference Fourier map is very useful for correcting the position of an atom used in structure factor calculation. This is also very useful in locating H-atoms towards the final stages of refinement procedure.

An analytical method of refinement of great power and generality is that based on the principle of least squares. In brief, least-squares refinement consists in using the squares of the differences between observed and calculated structure factors as a measure of their disagreement and adjusting the parameters so that the total disagreement is a minimum.

An agreement between the calculated structures factors F_c and those observed, F_o, indicates the degree of refinement. The most common method of assessing the agreement is calculating the residual or reliability index of the form

$$R = \frac{\sum(|F_o| - |F_c|)}{\sum|F_o|} \qquad 2.61$$

the summation being over all the reflections. Evidently, the lower the value of R, the better is the agreement. Another form of the residual of common use is

$$R_w = \left[\frac{\sum w(|F_o - F_c|^2)}{\sum w|F_o|^2}\right]^{\frac{1}{2}} \qquad 2.62$$

where the frequently used weight is, $w = \frac{1}{\sigma^2(F_o)}$

$\sigma(F_o)$ being the standard deviation of F_o.

After determining the structure with a reasonably low R-value various parameter of interest viz bond lengths, bond angles, torsion angles, non bonded distance etc., are determined using standard techniques.